On the combined use of GW approximation and cumulant expansion in the calculations of quasiparticle spectra: The paradigm of Si valence bands

Branko Gumhalter,[1,*] Vjekoslav Kovač,[2] Fabio Caruso,[3] Henry Lambert,[3] and Feliciano Giustino[3]
[1]*Institute of Physics, HR-10000 Zagreb, Croatia*
[2]*Department of Mathematics, University of Zagreb, HR-10000 Zagreb, Croatia*
[3]*Department of Materials, University of Oxford, Parks Road, Oxford OX1 3PH, United Kingdom*
(Received 15 February 2016; revised manuscript received 27 April 2016; published 5 July 2016)

Since the earliest implementations of the various GW approximations and cumulant expansion in the calculations of quasiparticle propagators and spectra, several attempts have been made to combine the advantageous properties and results of these two theoretical approaches. While the GW-plus-cumulant approach has proven successful in interpreting photoemission spectroscopy data in solids, the formal connection between the two methods has not been investigated in detail. By introducing a general bijective integral representation of the cumulants, we can rigorously identify at which point these two approximations can be connected for the paradigmatic model of quasiparticle interaction with the dielectric response of the system that has been extensively exploited in recent interpretations of the satellite structures in photoelectron spectra. We establish a protocol for consistent practical implementation of the thus established GW + cumulant scheme and illustrate it by comprehensive state-of-the-art first-principles calculations of intrinsic angle-resolved photoemission spectra from Si valence bands.

DOI: 10.1103/PhysRevB.94.035103

I. INTRODUCTION

In the past two decades a number of attempts have been made to combine the algorithms developed for calculating the band structure and quasiparticle properties in solids within the so-called GW approximations (GWAs) for the quasiparticle self-energy [1–12] with the powerful cumulant expansion or linked cluster approach [13–19] used for treating multiple excitation processes in the coupled quasiparticle-heat-bath systems [20–44]. The major rationale for combining these two approaches in the treatment of spectral properties of multiply excited systems stems from the empirically verified property of GWA to describe well the quasiparticle spectrum at the excitation threshold, on the one hand, and of cumulant expansion to reliably reproduce the multiexcitation structures where GWA fails, on the other hand. Here the relevant comparisons and assessments of the performance of two methods are made for the same generic interaction. In the GWA this is the dynamically screened electronic interaction W calculated in the the linear response. The ensuing cumulant approach is generated by the dynamic component of the same interaction which has the properties of a boson propagator. Thereby the problem maps onto the treatment of the coupled quasiparticle-boson system. The transition from all-electron to quasiparticle-boson model in the context of cumulant approach was discussed in Refs. [18,19,27].

In the context of *ab initio* calculations cumulant expansion was first employed in combination with the GW approximation to study the satellites in the photoemission spectra of simple metals [30]. Subsequent studies revealed that this approach may also prove useful to describe the plasmon satellites of silicon [35,45], graphene [37,46], and model systems [38,39]. Recently, the application of cumulant expansion to the calculation of angle-resolved spectral function of simple semiconductors highlighted the dispersive character of plasmonic satellites [41]. In particular, it was found that the simultaneous excitation of a plasmon and a hole leads to the emergence of "plasmonic polaron bands," which are broadened replicas of the valence bands blueshifted by the plasmon energy. This observation was recently confirmed by theoretical and experimental work [42,43,47]. These recent developments call for a detailed analysis of cumulant expansion, as well as its relation to the standard GWA.

The inequivalence of the results of GWA and cumulant approaches was demonstrated already in their earliest applications to the paradigmatic problem of photoemission spectra of core holes coupled to the linear electronic response of the medium [2] for which cumulant expansion provides the exact solution [18]. The existence of exact solution also made it possible to estimate the error incurred by the application of a concrete form of GWA. In the studied core hole case [2] the GWA solution was obtained from self-consistent calculation of the second-order self-energy induced by the dynamically screened Coulomb interaction W in the electron gas, and on the complete neglect of vertex corrections induced by W. This produced a compound structure in the core hole spectrum consisting of a narrow quasielastic peak at the blueshifted core hole spectral threshold and a much broader satellite or "plasmaron" structure starting at plasmon frequency ω_p below the threshold and reaching the maximum further down at approximately $2\omega_p$ (cf. Fig. 2 in Ref. [18]).

In contrast to the GWA, the second-order cumulant expansion provides an exact multiexcitation solution for the spectrum of a core hole coupled to the bosonlike dynamic component of W [18]. The obtained spectral structure exhibits the blueshifted main quasiparticle peak that is followed by a series of satellites located at redshifted multiples of the plasmon excitation energy. All spectral peaks exhibit infrared asymmetric broadening arising from the multiple

*Corresponding author: branko@ifs.hr

 ©2016 American Physical Society

excitation of low-energy electron-hole (e-h) pairs present in the dielectric response of electron gas (cf. Fig. 4 in Ref. [18]). Comparison of the cumulant and GWA solutions shows that the latter has the effect of forcing all the satellite peaks into a single one centered at the energy exceeding the plasmon excitation threshold by a factor $\geqslant 1.5$ and carrying their total weight. This fundamental difference between the two types of spectra arises from the different classes of processes the two approaches take into account. Cumulant expansion treats the processes described by boson-induced self-energy and vertex corrections on equivalent footing to all orders in the interaction and correlation between the successive scattering events. By contrast, the GWA solutions take into account only the self-energy corrections, either to lowest order(s) [24] or self-consistently to all orders in the noncrossing boson interaction lines [48], thereby leaving out all vertex corrections with crossing boson lines. This means that in order to exploit the results of GWA calculations for construction of cumulants, special care must be taken to select the appropriate GWA form which does not lead to overcounting of correlated higher-order self-energy-like contributions in cumulant expansion. This requires unambiguous identification of the levels of approximation at which GWA and cumulant expansion can be connected. Such a procedure is discussed in the forthcoming sections on the example of a single quasiparticle propagating in band states in which it is subject to the screened interaction W.

While cumulant expansion has been discussed in previous works (cf. Refs. [17,23,24,27,29,32,36], given the renewed interest in this technique and its use in conjunction with the GWA [29,30,35,37,41–44], it seems appropriate and timely to systematically develop and discuss the key aspects of the GW + cumulant (GW + C) theory for interpretations of the results of both the stationary and time-resolved spectroscopies. This program is carried out in Secs. II–V and critically assessed in Sec. VI. For the benefit of GW practitioners who may want to directly employ the results of the presented formalisms without going into the details of its derivation, we outline in Sec. VII a protocol for a consistent combined use of the *ab initio* GWA and cumulant expansion generated by the same dynamic interaction. Finally, as an illustrative example of the power of the developed approach, we apply it in Sec. VIII to investigate the effects of electron interactions with the charge density fluctuations in the spectral function of silicon.

II. PROPAGATORS OF QUASIPARTICLES AND BOSONIZED RESPONSE OF THE SYSTEM

A large class of many-body problems involving the interactions of quasiparticles (electrons or holes) with excitations in solids can be mapped onto the paradigmatic model of quasiparticle interactions with bosons. The justification for applying this model in the present studies of quasiparticles coupled to electronic excitations via the screened interaction W is the bosonic character of its dynamic component [34,44]. Since our attention is focused on excitations with energies ranging over the entire bandwidths we assume zero temperature of the system. Generalization to finite temperatures is a well-established procedure.

The generic Hamiltonian of the interacting particle-boson system reads

$$H = H^0_{\rm qp} + H^0_{\rm bos} + \lambda V = H^0 + \lambda V. \tag{1}$$

We express the components of (1) in the second quantization form in terms of the fermion creation and annihilation operators $c^\dagger_{\mathbf{k}}$ and $c_{\mathbf{k}}$ for the electron state with momentum $\mathbf{k}$, respectively, and the boson creation and annihilation operators $a^\dagger_{\mathbf{q},j}$ and $a_{\mathbf{q},j}$ for the state of the jth mode with wave vector $\mathbf{q}$, respectively. Using these operators we have for the unperturbed Hamiltonian of the quasiparticles

$$H^0_{\rm qp} = \sum_{\mathbf{k}} \epsilon^0_{\mathbf{k}} c^\dagger_{\mathbf{k}} c_{\mathbf{k}}, \tag{2}$$

where $\epsilon^0_{\mathbf{k}}$ in the unperturbed band-state energy. The Hamiltonian of unperturbed bosons is

$$H^0_{\rm bos} = \sum_{\mathbf{q},j} \omega_{\mathbf{q},j} a^\dagger_{\mathbf{q},j} a_{\mathbf{q},j}, \tag{3}$$

where $\omega_{\mathbf{q},j}$ is the energy (dispersion) of the jth mode. The particle-boson interaction is given by

$$\lambda V = \lambda \sum_{\mathbf{k},\mathbf{q},j} V^j_{\mathbf{k}-\mathbf{q},\mathbf{k}} c^\dagger_{\mathbf{k}-\mathbf{q}} c_{\mathbf{k}} a^\dagger_{\mathbf{q},j} + \text{H.c.} \tag{4}$$

Spectral properties of quasiparticles (electrons and holes) whose dynamics is governed by the Hamiltonian (1) are most conveniently obtained from the diagonal component of a causal (time-ordered) quasiparticle propagator or Green's function $G_{\mathbf{k}}(t,t')$. At zero temperature this is defined by [17,49–51]

$$\begin{aligned} G_{\mathbf{k}}(t,t') &= -i\langle 0|T[c_{\mathbf{k}}(t)c^\dagger_{\mathbf{k}}(t')]|0\rangle = -i\theta(t-t')\langle 0|c_{\mathbf{k}}(t)c^\dagger_{\mathbf{k}}(t')|0\rangle \\ &\quad + i\theta(t'-t)\langle 0|c^\dagger_{\mathbf{k}}(t')c_{\mathbf{k}}(t)|0\rangle \qquad (5) \\ &= -i\theta(t-t')\int_0^\infty d\omega \mathcal{N}^>_{\mathbf{k}}(\omega) e^{-i(\omega+\mu)(t-t')} \\ &\quad + i\theta(t'-t)\int_0^\infty d\omega \mathcal{N}^<_{\mathbf{k}}(\omega) e^{i(\omega-\mu)(t-t')}, \qquad (6) \end{aligned}$$

where $|0\rangle$ denotes the ground state of the system, the operators $c^\dagger_{\mathbf{k}}(t')$ and $c_{\mathbf{k}}(t)$ are expressed in the Heisenberg picture, and T is the time-ordering operator. The first term in (5) describes the probability amplitude that the electron created (injected) at time instant t' in an initially unoccupied eigenstate $|\mathbf{k}\rangle$ of the unperturbed Hamiltonian H^0 of the system is found in the same state at a later instant t. The second term gives the analogous probability for the hole created in an initially occupied state $\mathbf{k}$ at instant t to be found in the same state at a later instant t'. Here $\mathcal{N}^>_{\mathbf{k}}(\omega)$ and $\mathcal{N}^<_{\mathbf{k}}(\omega)$ are the spectral densities of the particle and the hole, respectively, and μ is the chemical potential. In the absence of interactions of quasiparticles with the heat bath (4) the noninteracting quasiparticle Green's function reads

$$\begin{aligned} G^{(0)}_{\mathbf{k}}(t-t') &= -i\theta(t-t')e^{-i(\epsilon^0_{\mathbf{k}}-i\eta)(t-t')}(1-n_{\mathbf{k}}) \\ &\quad + i\theta(t'-t)e^{-i(\epsilon^0_{\mathbf{k}}+i\eta)(t-t')}n_{\mathbf{k}}, \end{aligned} \tag{7}$$

where $n_{\mathbf{k}} = \langle 0|c^\dagger_{\mathbf{k}}c_{\mathbf{k}}|0\rangle$ is the occupation number of the one-particle $\mathbf{k}$ states in the ground state $|0\rangle$ and $\eta = 0^+$. This yields the Fourier transform (FT) of the unperturbed Green's function

in the form

$$G_{\mathbf{k}}^{(0)}(\omega) = \frac{1-n_{\mathbf{k}}}{\omega-\epsilon_{\mathbf{k}}^{0}+i\eta} + \frac{n_{\mathbf{k}}}{\omega-\epsilon_{\mathbf{k}}^{0}-i\eta}. \quad (8)$$

In the following we consider systems containing a *single* quasiparticle coupled to bosons. Since a single quasiparticle cannot give rise to renormalization of the boson field [17], the propagator $D_{\mathbf{q}}(t-t')$ of the $(\mathbf{q},j)$th boson mode in the system described by (1) should be equal to the unrenormalized one which at zero temperature takes a simple form [17],

$$D_{\mathbf{q},j}^{(0)}(t-t') = -i\theta(t-t')e^{-i\omega_{\mathbf{q},j}(t-t')} - i\theta(t'-t)e^{i\omega_{\mathbf{q},j}(t-t')}. \quad (9)$$

However, in view of the forthcoming discussions of bosonic excitations of the electron gas, we must assume a more general form,

$$D_{\mathbf{q}}(t-t') = -i\theta(t-t')\int_0^\infty d\omega' \mathcal{D}_{\mathbf{q}}(\omega')e^{-i\omega'(t-t')} - i\theta(t'-t)\int_0^\infty d\omega' \mathcal{D}_{\mathbf{q}}(\omega')e^{i\omega'(t-t')}, \quad (10)$$

where $\mathcal{D}_{\mathbf{q}}(\omega')$ is the mode density of bosonized heat-bath excitations of wave vector $\mathbf{q}$ that lie in the energy interval $d\omega'$ around ω'. Thus, for quasiparticle interactions with the heat bath represented by the surrounding electron liquid, this is obtained from the imaginary part of the corresponding electron density-density response function $\chi_{\mathbf{q}}(\omega')$, viz. $\mathcal{D}_{\mathbf{q}}(\omega') = \frac{1}{\pi}|\mathrm{Im}\chi_{\mathbf{q}}(\omega')|$. In this case we also have $V^{j}_{\mathbf{k}-\mathbf{q},\mathbf{k}} = V_{\mathbf{k}-\mathbf{q},\mathbf{k}}$. The thus formulated model describes equally well the propagation of quasiparticles in the bulk and in the quasi-two-dimensional (Q2D) surface bands where they couple also to surface localized excitations (surface plasmons, surface phonons, etc.) [36,52].

Expressions (8) and (10), together with the interaction matrix elements $V_{\mathbf{k}-\mathbf{q},\mathbf{k}}$, represent the point of departure for calculations of $G_{\mathbf{k}}(t-t')$ renormalized by the interactions with bosonized electronic excitations in the system. Its FT yields the $\mathbf{k}$-resolved quasiparticle spectrum

$$\mathcal{N}_{\mathbf{k}}(\omega) = \frac{1}{\pi}|\mathrm{Im}G_{\mathbf{k}}(\omega)| = \mathcal{N}_{\mathbf{k}}^{>}(\omega)\theta(\omega-\mu) + \mathcal{N}_{\mathbf{k}}^{<}(\omega)\theta(\mu-\omega). \quad (11)$$

The knowledge of (11) is needed in the determination of the various experimentally observable properties of the coupled quasiparticle-boson system. A characteristic example are photoemission yields from occupied electronic states of atomic, molecular, and condensed-matter systems which are directly related to the spectra of photoexcited holes [17,18,21,22,27,31,52–54].

Several methods of renormalization of (7) by the interaction with bosons (10) to yield (6) have been followed in the literature. The standard procedure is based on the expansion of $G_{\mathbf{k}}$ in Dyson series involving the proper self-energy corrections $\Sigma_{\mathbf{k}}$ in ascending powers of the interaction [17,49–51]. Here one of the most popular approximation schemes is the GW approximation in which the quasiparticle self-energy beyond the first order is represented by Feynman diagrams involving only noncrossing boson interaction lines (10). Depending on the complexity of the problem and the level of approximation [5], the effective number of interaction lines may range from one [1,2,24] to infinity in the self-consistent (SC) calculations [1,48,55]. The GWA results are considered to reliably reproduce the spectrum (11) near the quasiparticle excitation threshold, whereas they have been shown to be inadequate in the description of inelastic wings or satellite region [18,30]. To remedy this deficiency of GWA, another powerful method based on cumulant expansion [13,16] has been considered. The major rationale for this approach lies in the fact that cumulant expansion provides exact solutions in the limiting cases of (1) [18], or a rapidly converging closed-form solution in the general case [23,27,32,36]. Advantageous features of both approaches have been combined by a number of authors who have employed the GWA self-energies as an input for cumulant representation of quasiparticle propagators so as to achieve a better description of satellite structure in the spectra [27,29,30,33–37,41–44]. However, an explicit identification of the approximations underlying the combined use of GWA and cumulant expansion is still missing. In the following sections we make such a connection clear by using the model Hamiltonian (1).

The identification of a contact or "seam" between the GWA and the cumulant expansion in a joint GW + C approach can be most clearly identified by resorting to a system for which a closed-form solution for $G_{\mathbf{k}}(t,t')$ is available. Following this argument, we analyze in the following the propagation of a *single* quasiparticle whose dynamics is governed by the Hamiltonian (1) [36]. In effect, this means that the considered electron (hole) is injected into an empty (occupied) band or into a state sufficiently above (below) the Fermi level. This simplification introduces two important consequences in the propagators (5) and (8) describing the motion of quasiparticles.

(i) The quasiparticle propagates only in one time direction; i.e. only one term survives in (5), either the first one describing particles and proportional to $\theta(t-t')$ [implying the survival of only the first term in (8) with $n_{\mathbf{k}}=0$] or the second one for holes and proportional to $\theta(t'-t)$ [implying analogously the survival of only the second term in (8) with $n_{\mathbf{k}}=1$].

(ii) As a consequence of (i) all the quasiparticle-boson interaction vertices are restricted to the interval of quasiparticle propagation (t,t').

Subject to these conditions, cumulant expansion provides a tractable and asymptotically exact closed-form solution for the quasiparticle propagators (see Sec. IV below), which then allows equally tractable comparison with the results of GWA approach.

III. QUASIPARTICLE SELF-ENERGY IN THE G_0W_0 APPROXIMATION

A convenient representation of the general solution for Green's function (5) in the case of homogeneous and conservative systems is usually formulated for its Fourier transform $G_{\mathbf{k}}(\omega)$. The integral Dyson equation for a diagonal Green's function in the four-coordinate space transforms into an algebraic equation in the reciprocal $(\mathbf{k},\omega)$ space, where it can

be represented in the form [17,49–51]

$$G_{\mathbf{k}}(\omega) = G^{(0)}_{\mathbf{k}}(\omega) + G^{(0)}_{\mathbf{k}}(\omega)\Sigma_{\mathbf{k}}(\omega)G_{\mathbf{k}}(\omega). \tag{12}$$

Here the proper self-energy $\Sigma_{\mathbf{k}}(\omega)$ is given by the sum of all irreducible components involving the powers of interactions that perturb the initial noninteracting Hamiltonian H^0.

In the first application of GWA the lowest term of proper self-energy of the interacting electron gas was written "on the energy shell" $\omega = \epsilon^0_{\mathbf{k}}$ in the form [56]

$$\begin{aligned}\Sigma^{G_0W_0}_{\mathbf{k}}(\epsilon^0_{\mathbf{k}}) &= \int \frac{d^3q}{(2\pi)^3}\int \frac{d\omega'}{2\pi} G^{(0)}_{\mathbf{k}-\mathbf{q}}(\omega-\omega')W^{(0)}_{\mathbf{q}}(\omega'))\Big|_{\omega=\epsilon^0_{\mathbf{k}}} \\ &= \int \frac{d^3q}{(2\pi)^3}\int \frac{d\omega'}{2\pi}\frac{v_{\mathbf{q}}}{\varepsilon_{\mathbf{q}}(\omega')}\frac{1}{\omega-\omega'-\epsilon^0_{\mathbf{k}-\mathbf{q}}\pm i\eta}\Big|_{\omega=\epsilon^0_{\mathbf{k}}},\end{aligned} \tag{13}$$

and subsequently elaborated "off the energy shell" [1] and termed G_0W_0 self-energy [5]. Here $G^{(0)}$ denotes the unperturbed propagator of the electron or hole with $\pm i\eta$ in the denominator, respectively, and

$$W^{(0)}_{\mathbf{q}}(\omega') = v_{\mathbf{q}}/\varepsilon_{\mathbf{q}}(\omega') \tag{14}$$

stands for the matrix element of the bare Coulomb interaction $v_{\mathbf{k}-\mathbf{q},\mathbf{k}} = v_{\mathbf{q}}$ linearly screened by the dielectric function of the electron gas $\varepsilon_{\mathbf{q}}(\omega')$.

Using (13) as a point of departure, we can invoke the definition of dielectric function in the linear response formalism and write (14) in the form

$$W^{(0)}_{\mathbf{q}}(\omega') = v_{\mathbf{q}} + v_{\mathbf{q}}\chi_{\mathbf{q}}(\omega')v_{\mathbf{q}}, \tag{15}$$

where $\chi_{\mathbf{q}}(\omega')$ is the electronic density-density response function calculated in the standard random-phase approximation (RPA) or one of its generalized versions [44]. Now it is easy to verify that the function $\chi_{\mathbf{q}}(\omega')$ calculated within the linear response formalism has the properties of a boson propagator (10) with the spectrum of excitations given by $\mathcal{D}_{\mathbf{q}}(\omega') = (1/\pi)|\mathrm{Im}\chi_{\mathbf{q}}(\omega')|$ [33]. This makes it possible to represent the off-the-energy-shell form of expression (13) as

$$\Sigma^{G_0W_0}_{\mathbf{k}}(\omega) = \Sigma^{(1)}_{\mathbf{k}} + \Sigma^{(2)}_{\mathbf{k}}(\omega). \tag{16}$$

The first component on the right-hand side (RHS) of (16) reads

$$\Sigma^{(1)}_{\mathbf{k}} = \int \frac{d^3q}{(2\pi)^3} v_{\mathbf{q}} \int \frac{d\omega'}{2\pi} G^{(0)}_{\mathbf{k}-\mathbf{q}}(\omega-\omega') \tag{17}$$

and represents the ω-independent Fock-like correction equal to the first-order exchange self-energy [17]. This static contribution can be associated with other static contributions that renormalize $\epsilon^0_{\mathbf{k}}$, but it will be of no further interest in the context of dynamical particle-boson interactions studied within the cumulant approach. On the other hand, the second component (upper and lower signs stand for electrons and holes, respectively),

$$\Sigma^{(2)^{\gtrless}}_{\mathbf{k}}(\omega) = \int \frac{d^3q}{(2\pi)^3}\int d\omega' \frac{v^2_{\mathbf{q}}\mathcal{D}_{\mathbf{q}}(\omega')}{\omega-\epsilon^0_{\mathbf{k}-\mathbf{q}}\mp\omega'\pm i\eta}, \tag{18}$$

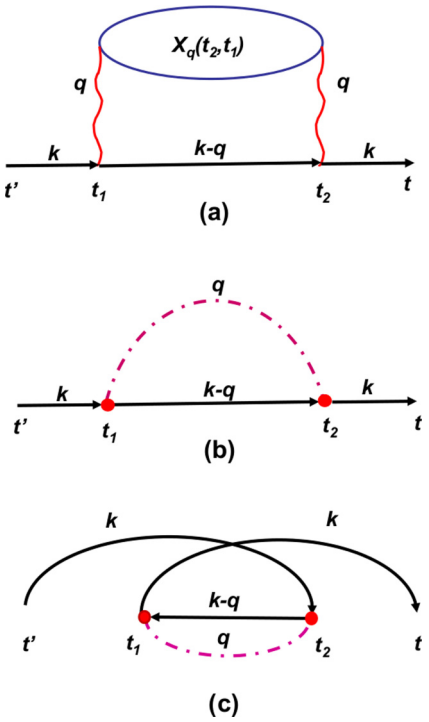

FIG. 1. (a) Diagram for the second-order contribution in the expansion of a Green's function (5) of an electron injected with the initial wave vector $\mathbf{k}$ into an empty band. Solid lines denote the unperturbed propagators, wavy lines denote the unscreened Coulomb interaction, and the bubble denotes the electronic response function $\chi_{\mathbf{q}}(t_2,t_1)$ of the system. (b) Equivalent diagram in the quasiparticle-boson model outlined in Sec. II. Solid circles denote the interaction matrix element $v_{\mathbf{q}}$ from Eq. (15) and the dash-dotted line denotes the boson propagator $D_{\mathbf{q}}(t_2-t_1)$ in the intermediate state interval (t_1,t_2). (c) Example of a second-order diagram involving two electrons above and one hole below the Fermi level in the same interval. This term cannot be generated within the single-particle limit of the Hamiltonian (1).

is dynamic as it gives ω-dependent contribution to (16) shown diagrammatically in the time domain as a self-energy insertion in Fig. 1(a). This has also been referred to as the correlation part or polarization contribution in Refs. [6] and [8], respectively. Therefore, the term (18) can be considered as describing the quasiparticle (electron or hole) interaction with the field of bosonized excitations of the surrounding electron gas. This passage is illustrated in Figs. 1(a)–1(c).

Expressions (13)–(18) enable us to establish a rigorous correspondence between the partial solution of the problem of dynamic interactions of a quasiparticle obtained within the GWA and cumulant approach. We note that it is also possible to extend the G_0W_0 approximation by dressing $G^{(0)}$ through the self-energy insertions induced by $W^{(0)}$ and solve self-consistently the equation for the thus-defined G [5,48]. First-principles calculations using the self-consistent GW formalism were reported in Refs. [57–61]. However, we demonstrate in the next sections that the results of such higher-order renormalizations cannot be mapped onto the standard cumulant expansion in ascending powers of the coupling constant λ [13,17]. Hence, they should not be pursued in the combined GW + C treatment of quasiparticle propagators.

IV. SINGLE-QUASIPARTICLE PROPAGATORS FROM CUMULANT EXPANSION

A. Cumulant expansion for a coupled particle-boson system

The dynamics of a quasiparticle injected into a state in an empty band state of the system is conveniently extracted from the quasiparticle propagator (22). Here we follow the notation and conventions of Refs. [16] and [17] and, for the sake of easier visualization, derive first the cumulants for electron propagators in the time domain. The cumulants for the propagators describing hole dynamics in occupied bands are derived by analogy in Sec. IV C.

We start from the Hamiltonian (1) and assume that the eigenstates $\{|\mathbf{k}\rangle\}$ of H_0 which define the initial one-electron band structure of the system are known, i.e., that this part of the problem has been solved first. In the single-particle limit the ground-state average in (5) can be conveniently calculated by using two standard hints. First, on noticing that before the injection of the particle into a band state described by the quantum number $\mathbf{k}$, one has $H|0\rangle = H^0|0\rangle = E^0|0\rangle$. This is in contrast to many-particle systems in which the initial ground state $|0\rangle$ is also renormalized by the interaction λV. Second, the evolution operator governing the time dependence of the operators $c_{\mathbf{k}}^{\dagger}(t) = e^{iHt}c_{\mathbf{k}}^{\dagger}e^{-iHt}$ and $c_{\mathbf{k}}^{\dagger}(t) = e^{iHt}c_{\mathbf{k}}e^{-iHt}$ is represented in the form

$$e^{-iHt} = e^{-i(H^0+\lambda V)t} = U(t) = e^{-iH^0t}U_I(t). \tag{19}$$

Here $U_I(t) = e^{iH^0t}e^{-iHt}$ is the evolution operator in the interaction picture generated by the perturbation λV and satisfying the integral equation

$$U_I(t) = 1 - i\int_0^t dt' V_I(t')U_I(t'), \tag{20}$$

where $V_I(t') = e^{iH^0t'}\lambda V e^{-iH^0t'}$. Now, since the unperturbed single-particle Green's function in the absence of the interaction λV reads

$$G_{\mathbf{k}}^{(0)}(t-t') = -i\theta(t-t')e^{-i(\epsilon_{\mathbf{k}}^0 - i\eta)(t-t')}, \tag{21}$$

we can write the full single-particle Green's function (5)

$$G_{\mathbf{k}}(t-t') = G_{\mathbf{k}}^{(0)}(t-t')\langle\mathbf{k}|U_I(t-t')|\mathbf{k}\rangle, \tag{22}$$

where, in shorthand notation, $|\mathbf{k}\rangle = c_{\mathbf{k}}^{\dagger}|0\rangle$. Thus, the calculation of the single-particle propagator deriving from (5) reduces to the evaluation of the diagonal matrix elements of $U_I(t)$ in the unperturbed basis. Thereby a perturbative solution to (5) involves the unperturbed propagators (10) and (21) and the matrix elements of λV.

The evolution operator $U_I(t)$ can always be expressed in an exponential form [62] and the averages of such generalized exponential operators are most conveniently calculated by using cumulant expansion in powers of the coupling constant λ of the perturbation that generates $U_I(t)$ [13]. This gives [62,63]

$$\langle\mathbf{k}|U_I(t-t')|\mathbf{k}\rangle = e^{C_{\mathbf{k}}(t-t')} \tag{23}$$

and hence

$$G_{\mathbf{k}}(t-t') = G_{\mathbf{k}}^{(0)}(t-t')e^{C_{\mathbf{k}}(t-t')}. \tag{24}$$

In the present problem defined by the Hamiltonian (1) the cumulant function

$$C_{\mathbf{k}}(t-t') = \sum_{l=2}^{\infty} C_{\mathbf{k}}^{(l)}(t-t') \tag{25}$$

is an infinite ascending series of cumulants in even powers of λ, viz. $C_{\mathbf{k}}^{(l)}(t-t') \propto \lambda^l$. They can be evaluated by directly employing the cumulant averaging of time-ordered products of operators $V_I(t)$ [13,23,32], or by equating the λ^lth-order terms of the Dyson expansion for the Green's function on the left-hand side (LHS) with the same powers of expanded exponential on the RHS of Eq. (24) [17,28]. The series (25) can converge fast even for strong coupling provided the correlations between successive quasiparticle-boson scattering events in higher-order cumulants are small [64,65], e.g., under the conditions of small relative transfers of energy and momentum from or to the quasiparticle during its propagation [23,32,36]. This is a consequence of a general theorem [13] which states that higher-order cumulants are expressed as differences between correlated and uncorrelated averages of the time-ordered products of operators $V_I(t)$. Thus, in the limit of infinite quasiparticle mass, which is realized for holes created in deep core levels of solids or adsorbates, already the second-order cumulant provides an exact result to (24) and (25) [18,27,52]. This is in stark contrast to the standard Dyson expansion of the Green's function (or the corresponding self-energy), where such an additional small expansion parameter does not exist. This has a very important practical implication in that the approximate Green's function (24) calculated by including only a small number of low-order cumulants gives a very accurate result, whereas the Dyson expansion of similar accuracy usually requires an infinite number of terms.

From the general properties of the evolution operator (20) generated by the Hamiltonian (1) one derives the following relations [36] satisfied by the cumulants (25)

$$C_{\mathbf{k}}(0) = 0, \tag{26}$$

$$\dot{C}_{\mathbf{k}}(0) = 0, \tag{27}$$

where the dot denotes the time derivative. The properties (26) and (27) apply to the whole series (25) as well as separately to its constituents. Expression (26) reflects the conservation of the norm of the spectrum $\mathcal{N}_{\mathbf{k}}(\omega)$ (unitarity). Relation (27) is a consequence of the property $C_{\mathbf{k}}^{(l\geqslant 2)}(t\to 0) \propto t^l$ arising from the generating interaction (4) and reflects the conservation of the first moment of the spectrum $\mathcal{N}_{\mathbf{k}}(\omega)$ (zero work sum rule [19,36]).

For the quasiparticle-boson model interaction (4) the second-order cumulant $C_{\mathbf{k}}^{(2)}(t)$ can be readily calculated [36] and for further convenience and reference its explicit derivation is presented in Sec. IV B. Following the procedures outlined in Ref. [13], the contributions from higher, fourth-order cumulants were calculated in Refs. [23] and [32] for nondispersive and dispersive bosons, respectively, and for all reasonable values of the coupling constants they have in both cases been found negligible relative to the ones from second-order cumulants. This property has been widely assumed as a

general feature in all later modelings of single-quasiparticle interactions with bosonic-type excitations based on cumulant expansion [16,21,29,30,33,35–37,41–43]. This approach has also proved extremely useful in the descriptions of ultrafast phenomena that can be revealed by time-resolved electron spectroscopies [33,34,36,44,66].

At this point a note is in order on the use of unperturbed quasiparticle Hamiltonians $H_{\rm qp}$, which are diagonal on the Kohn-Sham (KS) one-particle state basis and thus embody the electronic exchange-correlation (xc) effects in the corresponding KS one-particle energies. In order to avoid in this case the overcounting of xc effects in Eqs. (24) and (25), one should introduce the first-order cumulant $C_{\mathbf{k}}^{(1)}(t-t')$ which subtracts these effects from the renormalized energies in $G_{\mathbf{k}}$. This is analogous to the treatment of static initial-state interactions described in Fig. 8(b) of Ref. [18] and in Sec. II B. of Ref. [34]. In the case of KS states obtained within the local-density approximation (LDA) scheme, this is achieved by extending (25) with the term

$$C_{\mathbf{k}}^{(1)}(t-t') = -i\left[-v_{\mathbf{k}}^{\rm xc}(t-t')\right], \tag{28}$$

where $v_{\mathbf{k}}^{\rm xc}$ is the diagonal matrix element of the local KS LDA exchange-correlation potential in the state $\mathbf{k}$. This gives a stationary contribution to the quasiparticle energy that can be associated with $\epsilon_{\mathbf{k}}^0$ in $G_{\mathbf{k}}^{(0)}$, thereby allowing further treatment of the dynamic features of cumulant expansion without limitations imposed on the unperturbed basis. Note in passing that the property (27) does not apply to the *ad hoc* added cumulant (28).

B. Second-order cumulant

The Feynman diagram corresponding to the second-order process in λV that is common to cumulant and Dyson expansion of Green's function (5) governed by (1) is shown in Fig. 1(b). It involves the unperturbed propagators (10) and (21) and the matrix elements $V_{\mathbf{k-q},\mathbf{k}}$ of the interaction V in the basis of quasiparticle and boson eigenfunctions diagonalizing H^0. For interactions (4) constrained to the interval (t',t), this gives the first nonvanishing correction to the unperturbed single-electron Green's function to order λ^2:

$$iG_{\mathbf{k}}^{(2)}(t-t') = \int_{t'}^{t} dt_2 \int_{t'}^{t} dt_1 iG_{\mathbf{k}}^{(0)}(t-t_2)\left[\sum_{\mathbf{q}}(-i\lambda V_{\mathbf{k-q},\mathbf{k}})^2 iD_{\mathbf{q}}(t_2-t_1) iG_{\mathbf{k-q}}^{(0)}(t_2-t_1)\right] iG_{\mathbf{k}}^{(0)}(t_1-t') \tag{29}$$

$$= iG_{\mathbf{k}}^{(0)}(t-t')\left[\sum_{\mathbf{q}}(-i\lambda V_{\mathbf{k-q},\mathbf{k}})^2 \int d\omega' \mathcal{D}_{\mathbf{q}}(\omega') \frac{1-e^{-i(\epsilon_{\mathbf{k-q}}^0+\omega'-\epsilon_{\mathbf{k}}^0)(t-t')} - i\left(\epsilon_{\mathbf{k-q}}^0+\omega'-\epsilon_{\mathbf{k}}^0\right)(t-t')}{(\epsilon_{\mathbf{k-q}}^0+\omega'-\epsilon_{\mathbf{k}}^0)^2}\right] \tag{30}$$

$$= iG_{\mathbf{k}}^{(0)}(t-t')C_{\mathbf{k}}^{(2)}(t-t'). \tag{31}$$

To obtain (30) and (31), we have exploited the single particle-imposed time ordering $t > t_2 > t_1 > t'$. The thus-obtained $G_{\mathbf{k}}^{(2)}(t-t')$ serves as a definition of the second-order self-energy given in the time domain through the expression in the square brackets on the RHS of (29) and of the second-order cumulant generated by the same interaction and given by expression in the square brackets in (30). Respectively, they are given by the expression

$$-i\Sigma_{\mathbf{k}}^{(2)}(t_2-t_1) = \sum_{\mathbf{q}}(-i\lambda V_{\mathbf{k-q},\mathbf{k}})^2 iD_{\mathbf{q}}(t_2-t_1) iG_{\mathbf{k-q}}^{(0)}(t_2-t_1), \tag{32}$$

which constitutes the diagram in Fig. 1(b) and whose FT yields (18), and

$$C_{\mathbf{k}}^{(2)}(t-t') = -\sum_{\mathbf{q}}(\lambda V_{\mathbf{k-q},\mathbf{k}})^2 \int d\omega' \mathcal{D}_{\mathbf{q}}(\omega') \frac{1-e^{-i(\epsilon_{\mathbf{k-q}}^0+\omega'-\epsilon_{\mathbf{k}}^0)(t-t')} - i\left(\epsilon_{\mathbf{k-q}}^0+\omega'-\epsilon_{\mathbf{k}}^0\right)(t-t')}{\left(\epsilon_{\mathbf{k-q}}^0+\omega'-\epsilon_{\mathbf{k}}^0\right)^2}. \tag{33}$$

The factorization appearing in the last line of (31) is a direct consequence of the simple exponential form of unperturbed $G_{\mathbf{k}}^{(0)}(t)$ given by (21), which allows propagation in one time direction only. Such a factorization can be established in all orders of perturbation and enables the rearrangement of the Dyson series for a single-particle propagator into a product of $iG_{\mathbf{k}}^{(0)}(t-t')$ and the terms that can be directly related to exponentiated sum of cumulants (25) [17,28]. We stress that this property does not generally hold for causal, time-ordered quasiparticle propagators; therefore, time-ordered propagators cannot be represented in simple cumulant form. This implies that the use of the cumulant expansion is fully justified only when considering the quasiparticle Green's functions propagating in one time direction only [15,18,21,23,27,32,36,38].

Another important property of the thus-derived $G_{\mathbf{k}}^{(2)}(t-t')$ is the absence of the factor $i\eta$ from explicit expression for $C_{\mathbf{k}}^{(2)}(t-t')$ and its presence only in the factorized term $G_{\mathbf{k}}^{(0)}(t-t')$. This is due to cancellations of exponents in the products of factors $e^{-\eta t_j}e^{+\eta t_j}$ arising from two successive $G_{\mathbf{k}}^{(0)}$s in each jth interaction vertex. Note that for this to occur η need not be infinitesimal but only constant. Therefore, in order to study the temporal properties of $C_{\mathbf{k}}^{(2)}(t-t')$, it would be *inappropriate* to introduce at the outset the factor $i\eta$ into the denominator on the RHS of (33), the more so because the whole expression is nonsingular for $(\epsilon_{\mathbf{k-q}}^0+\omega'-\epsilon_{\mathbf{k}}^0)\to 0$. These subtle properties of $C_{\mathbf{k}}^{(2)}(t-t')$ are further elaborated below.

C. Integral representation of $C_{\mathbf{k}}(t-t')$

Expression (33) can be brought to a more compact form by making use of definition (10) and by introducing the interaction weighted joint density of excitations $\rho_{\mathbf{k}}^{(2)>}(\nu)$ for electron propagation with $\epsilon_{\mathbf{k}}^0$ and $\epsilon_{\mathbf{k}-\mathbf{q}}^0$ above the Fermi level [16,36]. Introducing the matrix elements $\lambda V_{\mathbf{k}-\mathbf{q},\mathbf{k}} = v_{\mathbf{k}-\mathbf{q},\mathbf{k}}$ we obtain by using (10) and (18)

$$\begin{aligned}\rho_{\mathbf{k}}^{(2)>}(\nu) &= \sum_{\mathbf{q}} v_{\mathbf{k}-\mathbf{q},\mathbf{k}}^2 (1-n_{\mathbf{k}})(1-n_{\mathbf{k}-\mathbf{q}}) \int_0^\infty d\omega' \mathcal{D}_{\mathbf{q}}(\omega') \\ &\quad \times \delta\left[\nu - \left(\omega' + \epsilon_{\mathbf{k}-\mathbf{q}}^0 - \epsilon_{\mathbf{k}}^0\right)\right] \\ &= -\frac{1}{\pi}\mathrm{Im}\Sigma_{\mathbf{k}}^{(2)>}\left(\epsilon_{\mathbf{k}}^0 + \nu\right). \end{aligned} \tag{34}$$

The thus-defined $\rho_{\mathbf{k}}^{(2)>}(\nu)$ is bounded from below at $\nu = -(\epsilon_{\mathbf{k}}^0 - E_{\mathrm{low}}) \leqslant 0$ when the particle is scattered to the lowest unoccupied state of energy E_{low}, which is the supremum of the band bottom energy $\epsilon_{\mathbf{k}-\mathbf{q}}^0 = 0$ and the Fermi energy $\epsilon_F = \mu$. The other limit $\rho_{\mathbf{k}}^{(2)>}(\nu \to \infty)$ is dictated by the asymptotic behavior of $\mathrm{Im}\chi_{\mathbf{q}}(\nu)$ [67].

In the case of single-hole propagation (symbol $<$) the corresponding joint density of excitations takes the form

$$\begin{aligned}&\rho_{\mathbf{k}}^{(2)<}(\nu) \\ &= \sum_{\mathbf{q}} v_{\mathbf{k}-\mathbf{q},\mathbf{k}}^2 n_{\mathbf{k}} n_{\mathbf{k}-\mathbf{q}} \int_0^\infty d\omega' \mathcal{D}_{\mathbf{q}}(\omega') \delta\left[\nu - \left(\omega' - \epsilon_{\mathbf{k}-\mathbf{q}}^0 + \epsilon_{\mathbf{k}}^0\right)\right] \\ &= \frac{1}{\pi}\mathrm{Im}\Sigma_{\mathbf{k}}^{(2)<}\left(\epsilon_{\mathbf{k}}^0 - \nu\right) \end{aligned} \tag{35}$$

and is lower bounded at $\nu = -(E_{\mathrm{up}} - \epsilon_{\mathbf{k}}^0) \leqslant 0$, where E_{up} is the infimum of the upper occupied band edge and ϵ_F.

Definitions (34) and (35) enable us to write the second-order cumulant for electron and hole propagation in a compact form,

$$\begin{aligned}C_{\mathbf{k}}^{(2)\gtrless}(t) &= -\int d\nu \rho_{\mathbf{k}}^{(2)\gtrless}(\nu) \frac{1 - e^{\mp i\nu t} \mp i\nu t}{\nu^2} \\ &= -\int d\nu \left[\mp \frac{1}{\pi}\Sigma_{\mathbf{k}}^{(2)\gtrless}\left(\epsilon_{\mathbf{k}}^0 \pm \nu\right)\right] \frac{1 - e^{\mp i\nu t} \mp i\nu t}{\nu^2}. \end{aligned} \tag{36}$$

Here it should be observed that $\rho_{\mathbf{k}}^{(2)\gtrless}(\nu)$ are not on-the-energy-shell quantities so that the energy conservation contained in $C_{\mathbf{k}}^{(2)\gtrless}(t)$ is determined solely by the properties of the long-time limit $t \to \infty$ of expression (36).

Although the integral representation (36) of the cumulant function has been here established for the second-order term in (25), it can be shown (see Sec. A of the Supplemental Material [68]) that the whole cumulant series (25) can be formally obtained through the mapping $\rho(\nu) \leftrightarrow C(t)$ using the same integral transform as in (36) [36], viz.,

$$C_{\mathbf{k}}^{\gtrless}(t) = -\int d\nu \rho_{\mathbf{k}}^{\gtrless}(\nu) \frac{1 - e^{\mp i\nu t} \mp i\nu t}{\nu^2}. \tag{37}$$

In both cases (hereafter in the present subsection we drop the superscripts $>$ and $<$)

$$\rho_{\mathbf{k}}(\nu) = \sum_{l=2}^{\infty} \rho_{\mathbf{k}}^{(l)}(\nu), \tag{38}$$

with $\rho_{\mathbf{k}}^{(l)}(\nu) \propto \lambda^l$ and where $\rho_{\mathbf{k}}^{(2)}(\nu)$ is the lowest term of the series from which (28) is excluded. Owing to the bijection properties of the integral transform (37), here each $\rho_{\mathbf{k}}^{(l)}(\nu)$ can be uniquely obtained from the inverse transform of the corresponding $C_{\mathbf{k}}^{(l)}(t)$ [36] defined by

$$\rho_{\mathbf{k}}^{(l)}(\nu) = -\frac{1}{2\pi}\int_{-\infty}^{\infty} \ddot{C}_{\mathbf{k}}^{(l)}(t) e^{i\nu t} dt, \quad l > 1, \tag{39}$$

where double dot denotes second-order time derivative. Expressions (37) and (38) also enable a compact semidiagonal representation of the initial Hamiltonian (1) in terms of particle interaction with *drag bosons* formulated in Sec. B of the Supplemental Material [68]. This representation facilitates direct constructions of the diagonal single-quasiparticle propagators (5) and cumulant series (25).

Despite the fact that (39) now extends the applicability of (36) to the entire series (25), it again poses the question of tedious derivations of higher-order cumulants and the ensuing $\rho_{\mathbf{k}}^{(l)}(\nu)$ by the standard cumulant expansion of the evolution operator [13,32]. Therefore, the importance of the general integral representation defined by (37)–(39), and proven in Sec. A of the Supplemental Material [68] is in the domain of the existential theorem for representation of the cumulant series generated by the Hamiltonian (1) and the discussion of its global properties in the various temporal intervals of physical relevance (see Sec. V). However, as pointed out in Sec. IV D, all higher-order terms give rise to negligible corrections in the case of systems that dynamicswise can be mapped to particle-boson model Hamiltonians with standard coupling strengths [23,32].

D. Range of validity and limitations of the second-order cumulant expansion

Cumulant expansion is of great practical importance for the class of problems or model systems for which the low-order cumulants provide either the full or the dominant contribution to the series (25). A typical example of the former case is the core hole problem described by (1) with the single core level Hamiltonian $H_c^0 = \epsilon_c^0 c_c^\dagger c_c$ and the factorized coupling of the hole density to the boson field, viz., $\lambda V \propto -c_c c_c^\dagger$ (see Refs. [18,52]). Here the sum of the first- and second-order cumulants provides an exact solution due to the absence of any correlations between the successive boson emission and absorption events because the source of perturbation on the boson field, i.e., the localized core hole, is dynamically structureless. Its only degree of freedom is its energy ϵ_c, which, likewise the matrix elements $v_{\mathbf{k}-\mathbf{q},\mathbf{k}} \to v_{\mathbf{q}}$, is not affected by the quasiparticle recoil in the boson excitation processes. This gives rise to cancellation of all higher-order cumulants which measure correlations among the interaction vertices [13] and to a reduction of cumulant series (25) to the second-order term (36). This feature has been successfully employed in the

interpretations of core level line shapes in the bulk [18,27] and at surfaces [52].

The above discussion gives a clue as to the validity of approximate treatment of the problem posed by quasiparticle-boson Hamiltonian (1). Inspection of the expressions for the fourth-order cumulants [23,32] shows that in the presence of translational invariance in the phase space which applies to the energy differences

$$\epsilon^0_{\mathbf{k+q+p}} - \epsilon^0_{\mathbf{k+q}} \leftrightarrow \epsilon^0_{\mathbf{k+p}} - \epsilon^0_{\mathbf{k}} \tag{40}$$

and to the interaction matrix elements

$$V_{\mathbf{k+q+p},\mathbf{k+q}} \leftrightarrow V_{\mathbf{k+p},\mathbf{k}}, \tag{41}$$

the fourth- and higher-order cumulants turn to zero. These invariances are characteristic of the absence of correlations between successive boson emission and reabsorption events. Hence, in the complete absence of such correlations, as is the case with boson fields perturbed either by structureless or classical time dependent potentials, the cumulant series (25) reduces to a single term given by the second-order cumulant (33) in which $V_{\mathbf{k-q},\mathbf{k}} \to V_{\mathbf{q}}$ and $\epsilon^0_{\mathbf{k-q}} - \epsilon^0_{\mathbf{k}} \to 0$. This exactly solvable limit of the particle-boson Hamiltonian is known as the forced oscillator model [16,17,69,70]. If the correlations are nonvanishing but small, then the second-order cumulant expansion provides a good approximation for the calculation of quasiparticle amplitudes (24) [23,32].

The translational invariances (40) and (41) are expected to hold well in two extreme situations. The first is the case of very large quasiparticle mass, or equivalently very narrow quasiparticle band, which is the core hole limit elaborated above. The second is the case of a very broad quasiparticle band and initial $\epsilon^0_{\mathbf{k}}$ far from the band edges (or from the Fermi level). In this case the variations of $\epsilon^0_{\mathbf{k}}$ may be considered to be nearly linear, and the variation of the matrix elements of λV nearly zero for small variations of the quantum number $|\mathbf{k}|$, which altogether makes all $C^{(l>2)}_{\mathbf{k}}(t)$ very small. Therefore, the convergence of the cumulant series (25) is system specific as it depends on the trade-off between the strength of the interaction (i.e., the magnitude of the coupling constant λ) and the correlations between successive scattering events.

Second-order cumulant expansion becomes increasingly worse as the quasiparticle energy moves closer to the band edges where correlations between subsequent scattering events induced by λV may become large. In this regime the low-order self-energy corrections may represent a better approximation to the quasiparticle propagator, particularly in relation to its asymptotic time behavior characterized by the so-called quasiparticle collapse [36,71–74]. Moreover, near the Fermi level the single-particle approximation which separates electron from hole motion and leads to (34) and (35) becomes unrealistic and the processes like those shown in Fig. 1(c) need be considered. In principle, there is no difficulty with their implementation because they also generate the same form of second-order cumulant provided t_1 and t_2 are restricted to the time interval (t',t), and the corresponding $\rho^{(2)^{\gtrless}}_{\mathbf{k}}(\nu)$ is also readily obtainable from the G_0W_0 self-energy contained in Fig. 1(c). Rather, the problem arises in that the analogous W-induced fluctuations across the Fermi surface exist also outside this interval and hence in a *consistent* approach should be coupled to the quasiparticle injected into the same region of the phase space. This leads to the standard, adiabatic formulation of Green's function (6) amenable to usual perturbation treatment which, in general, is not representable in cumulant form [21]. An analogous argument holds also for holes created near the Fermi surface. However, cumulant representation with *partly restored afore-required consistency* is regained by resorting to a hybrid approach in which the renormalization of one-particle states in the intervals $(-\infty,t')$ and (t,∞) is accounted for through their representation by stationary KS states and within the excitation interval (t',t) through *dynamical* renormalization by the generically same interaction W using cumulant expansion. The second-order cumulant is in this case generated by the full G_0W_0 self-energy, as implemented in [30] and extensively used thereafter. However, the degree of consistency of this matching near the Fermi level is not *a priori* clear and deviations from the standard Feynman-Dyson perturbation expansion remain to be explored.

V. TEMPORAL EVOLUTION OF THE AMPLITUDE AND PHASE OF THE QUASIPARTICLE PROPAGATOR

Using the closed-form solution (24) for the propagator in cumulant representation, one can introduce the quantities which conveniently measure temporal evolution of the quasiparticle upon its promotion into the initial state $|\mathbf{k}\rangle$. Again we first discuss the case of electron propagators and spectra and then deduce the corresponding quantities for holes. In this context the quantity of primary interest is the survival probability of the quasiparticle initial state,

$$L_{\mathbf{k}}(t) = \mid G_{\mathbf{k}}(t) \mid^2 = \exp[2\mathrm{Re}C_{\mathbf{k}}(t)], \tag{42}$$

and the evolution of its phase defined by

$$\phi_{\mathbf{k}}(t) = -\mathrm{Im}\ln[iG_{\mathbf{k}}(t)] = \epsilon^0_{\mathbf{k}}t - \mathrm{Im}C_{\mathbf{k}}(t) = \epsilon^0_{\mathbf{k}}t + \varphi_{\mathbf{k}}(t). \tag{43}$$

In this notation the derivative $\partial\varphi_{\mathbf{k}}(t)/\partial t$ describes the relaxation of quasiparticle energy in the course of time.

Of particular interest is the behavior of (42) and (43) on the various time scales characteristic of the studied system. Quite generally, the quasiparticle evolution generated by the Hamiltonian (1) and described by (42) and (43) exhibits three distinct consecutive stages [36]:

(i) early time non-Markovian evolution characterized by the initial off-the-energy-shell transients;

(ii) intermediate-stage quasistationary Markovian evolution characterized by the exponential decay of quasiparticle probability amplitude (42) and stationary derivative of the phase $\partial\varphi_{\mathbf{k}}(t)/\partial t$;

(iii) collapse of the quasiparticle amplitude and phase in the asymptotic limit $t \to \infty$.

The remainder of this section discusses the characteristics of these evolution regimes.

A. Initial transients and the crossover to quasistationary regime of quasiparticle propagation

The early quasiparticle propagation past its injection into the eigenstate $|\mathbf{k}\rangle$ of H^0 is before the establishment of

energy conservation governed by initial off-the-energy-shell transients. The first transient is the Zeno decay,

$$L_{\mathbf{k}}(t \to 0) = \exp\left(-t^2/\tau_Z^2\right), \tag{44}$$

where τ_Z is the so-called Zeno time, which measures the convexity of the initial drop of the amplitude of the quasiparticle during its earliest ballistic propagation in the band [75]. This is followed by virtual excitation of the modes that constitute the response of the heat bath described by H^0_{bos}. Since the coupling to coherent collective modes of the heat-bath-like plasmons is usually strong, the initial transients in (42) and (43) may be dominated by oscillations with the period of inverse plasmon frequency. The onset of steady-state quasiparticle propagation is governed by the establishment of energy conservation; this happens when the functionals $(1-\cos\nu t)/\nu^2$ and $\sin\nu t/\nu$ in the general integral representation of $C_{\mathbf{k}}(t)$ defined by (37) can be replaced with their equivalent long-time asymptotic forms $\pi\delta(\nu)|t|$ and $\pi\delta(\nu)$, respectively. Since this strongly depends on the structure of $\rho_{\mathbf{k}}(\nu)$ the onsets are very system specific. Illustrative examples of such specificities pertaining to holes excited in Q2D bands on Ag(111) and Cu(111) surfaces are presented in Figs. 4 and 5 of Ref. [44]. To grasp their emergence, it is of utmost importance to note that the description of establishment of steady-state propagation does not require the introduction of an additional infinitesimal $i\eta$ into the denominator of the integrand on the RHS of (37) as long as the oscillating terms are retained. Namely, the neglect of oscillatory terms and simultaneous introduction of $i\eta$ in the denominator is an auxiliary procedure in the treatments based on the assumption of *adiabatic* temporal boundary conditions. The latter are typical of the scattering experiments in which the projectile-target interaction is switched on and off adiabatically, whereas in the present problem we deal with the instantaneous switching on of λV that is typical of photoemission boundary conditions. It is only in the long-time or asymptotic limit that the two types of temporal boundary conditions may give the same results. In other words, the kernel of the integral transform on the RHS of (37), viz., the function $(1-e^{-i\nu t}-i\nu t)/\nu^2$, takes a proper account of the passage of the quasiparticle from the initial transient, energy nonconserving interval to a subsequent quasistationary regime of propagation in which the energy of the quasiparticle-boson system is conserved.

B. Quasistationary regime

1. *Polarization energy shift*

Once the quasistationary regime is reached one can single out from $C_{\mathbf{k}}(t)$ its imaginary part linear in t that determines the long-time behavior of $\varphi_{\mathbf{k}}(t)$ in (43). This gives the polarization or energy relaxation shift $\Delta_{\mathbf{k}}$ of the unperturbed level energy $\epsilon^0_{\mathbf{k}}$, viz.,

$$C^{\mathrm{pol}\gtrless}_{\mathbf{k}}(t) = -i\left[\mp\int d\nu\,\frac{\rho^{\gtrless}_{\mathbf{k}}(\nu)}{\nu}\right]t = -i\,\Delta^{\gtrless}_{\mathbf{k}}t. \tag{45}$$

The integral is taken in the sense of principal value with the range of integration extended over the whole bandwidth of $\rho^{\gtrless}_{\mathbf{k}}(\nu)$. This is in accord with the notion of polarization or relaxation energy involving all virtual, off-the-energy-shell excitations embodied in $\rho^{\gtrless}_{\mathbf{k}}(\nu)$. Thus, substituting the leading cumulant joint density of excitations $\rho^{(2)\gtrless}_{\mathbf{k}}(\nu)$ given by (34) and (35) into expression (45), one obtains the second-order Rayleigh-Schrödinger (RS) perturbation theory correction to the unperturbed quasiparticle energy $\epsilon^0_{\mathbf{k}}$ derived from expression (18), viz.,

$$\Delta^{(2)\gtrless}_{\mathbf{k}} = \mathrm{Re}\Sigma^{(2)\gtrless}_{\mathbf{k}}\left(\epsilon^0_{\mathbf{k}}\right) \propto \lambda^2, \tag{46}$$

and analogously so for the fourth-order terms $\propto\lambda^4$ [17]. This illustrates that the natural basis for cumulant representation (24) is the space spanned by the one-particle eigenstates and eigenenergies of H^0 [13,17], and not by any partially renormalized quantities (e.g., like those derived from SC Brillouin-Wigner perturbation theory), as that would lead to *overcounting* of the terms of the same powers in λ. This could have been inferred also from the explicit form of the second-order cumulant (33).

2. *Quasistationary propagation of recoiling quasiparticles*

The cumulant function $C_{\mathbf{k}}(t)$ may embody another contribution linear in t besides the purely imaginary term (45), yielding the polarization energy. This arises from the long-time limit of $(1-\cos\nu t)/\nu^2 \to \pi\delta(\nu)|t|$ in the integral representation of $C_{\mathbf{k}}(t)$ [cf. expression (37)], which is nonvanishing provided there exists a quasiparticle component $\rho^{\mathrm{qp}}_{\mathbf{k}}(\nu)$ of $\rho^{\gtrless}_{\mathbf{k}}(\nu)$ with smooth low-energy behavior,

$$\rho^{\mathrm{qp}}_{\mathbf{k}}(\nu \to 0) = \rho^{\mathrm{qp}}_{\mathbf{k}}(0) + \nu\partial\rho^{\mathrm{qp}}_{\mathbf{k}}(\nu)/\partial\nu|_{\nu=0}. \tag{47}$$

Such a quasistationary property of $\rho^{\mathrm{qp}}_{\mathbf{k}}(\nu)$ requires that the quasiparticle recoil energy $\epsilon^0_{\mathbf{k}-\mathbf{q}} - \epsilon^0_{\mathbf{k}}$ be degenerate with the continuum of heat-bath excitations like the electron-hole pairs, acoustic phonons, etc. This yields the long-time behavior of the quasiparticle component $C^{\mathrm{qp}}_{\mathbf{k}}(t)$ of $C_{\mathbf{k}}(t)$ comprising the terms linear in t and a complex constant, viz.,

$$\lim_{t\to\pm\infty} C^{\mathrm{qp}\gtrless}_{\mathbf{k}}(t) = -i\left(\Delta^{\mathrm{qp}\gtrless}_{\mathbf{k}} \mp i\Gamma^{\mathrm{qp}\gtrless}_{\mathbf{k}}\right)t - w^{\mathrm{qp}\gtrless}_{\mathbf{k}}. \tag{48}$$

Here

$$\Gamma^{\mathrm{qp}\gtrless}_{\mathbf{k}} = \pi\rho^{\mathrm{qp}\gtrless}_{\mathbf{k}}(0) \tag{49}$$

has the meaning of the quasiparticle decay rate per unit time and is an on-the-energy-shell quantity, in contrast to the polarization energy $\Delta^{\mathrm{qp}\gtrless}_{\mathbf{k}}$. The structure of the complex constant $w^{\mathrm{qp}\gtrless}_{\mathbf{k}}$, which derives from quasistationary $\rho^{\mathrm{qp}\gtrless}_{\mathbf{k}}(\nu)$ around the excitation threshold $\nu = 0$, can be deduced by using the equivalence of long-time limits of the kernel of integral transformation (37) and its stationary representation

$$w^{\mathrm{qp}\gtrless}_{\mathbf{k}} = \lim_{t\to\pm\infty}\int d\nu\,\frac{1-e^{\mp i\nu t}}{\nu^2}\rho^{\mathrm{qp}\gtrless}_{\mathbf{k}}(\nu) \to \int d\nu\,\frac{\rho^{\mathrm{qp}\gtrless}_{\mathbf{k}}(\nu)}{(\nu\pm i\eta)^2}$$
$$= -\int d\nu\rho^{\mathrm{qp}\gtrless}_{\mathbf{k}}(\nu)\frac{\partial}{\partial\nu}\frac{1}{\nu\pm i\eta} = \int d\nu\,\frac{\frac{\partial}{\partial\nu}\rho^{\mathrm{qp}\gtrless}_{\mathbf{k}}(\nu)}{\nu\pm i\eta}. \tag{50}$$

In the case of second-order cumulants we substitute expressions (34) and (35) into (45) and (50), change the integration

variables, and use the Kramers-Kronig relations to obtain

$$\Delta_{\mathbf{k}}^{\mathrm{qp}^{\gtrless}} \mp i\Gamma_{\mathbf{k}}^{\mathrm{qp}^{\gtrless}} = \mathrm{Re}\Sigma_{\mathbf{k}}^{\mathrm{qp}^{\gtrless}}(\epsilon_{\mathbf{k}}^{0}) + i\mathrm{Im}\Sigma_{\mathbf{k}}^{\mathrm{qp}^{\gtrless}}(\epsilon_{\mathbf{k}}^{0}), \tag{51}$$

$$w_{\mathbf{k}}^{\mathrm{qp}^{\gtrless}} = -\frac{\partial}{\partial\nu}\Sigma_{\mathbf{k}}^{\mathrm{qp}^{\gtrless}}(\nu)|_{\nu=\epsilon_{\mathbf{k}}^{0}}. \tag{52}$$

Relations (48), (51), and (52) signify that the analytic properties of $G_{\mathbf{k}}^{\mathrm{qp}}(\omega)$ deriving from (48) are determined dominantly by the pole located at $\omega = \epsilon_{\mathbf{k}}^{0} + \Delta_{\mathbf{k}}^{\mathrm{qp}^{\gtrless}} \mp i\Gamma_{\mathbf{k}}^{\mathrm{qp}^{\gtrless}}$ in the complex plane, with the weight (residue) $Z_{\mathbf{k}} = \exp(-w_{\mathbf{k}}^{\mathrm{qp}^{\gtrless}})$. Note that other nonanalytic structures that may appear in the full $G_{\mathbf{k}}(\omega)$, e.g., like those associated with the cuts in complex plane, give rise to different temporal asymptotic behavior of $G_{\mathbf{k}}(t)$ that *cannot be represented by the simple form* (48) (see Sec. V C).

For later convenience we may generalize these results to several bands. This implies that all intermediate-state summations should also include allowed interband transitions $(\mathbf{k},n) \to (\mathbf{k}',n')$. Then the asymptotic behavior of the cumulants (48) and (28) produces a peak in the quasiparticle spectrum in the nth band described by

$$\mathcal{N}_{\mathbf{k},n}^{\mathrm{qp}^{\gtrless}}(\omega) = \frac{\binom{1-n_{\mathbf{k},n}}{n_{\mathbf{k},n}}}{\pi} \times e^{-w_{\mathbf{k},n}} \frac{[\Gamma_{\mathbf{k},n}\cos\alpha_{\mathbf{k},n} - (\omega - E_{\mathbf{k},n})\sin\alpha_{\mathbf{k},n}]}{(\omega - E_{\mathbf{k},n})^2 + \Gamma_{\mathbf{k},n}^2}, \tag{53}$$

where in the shorthand notation $w_{\mathbf{k},n} = \mathrm{Re}w_{\mathbf{k},n}^{\mathrm{qp}^{\gtrless}}$, $\alpha_{\mathbf{k},n} = \mathrm{Im}w_{\mathbf{k},n}^{\mathrm{qp}^{\gtrless}}$, $E_{\mathbf{k},n} = \epsilon_{\mathbf{k},n}^{0} + \Delta_{\mathbf{k},n}^{\mathrm{qp}^{\gtrless}} - v_{\mathbf{k},n}^{\mathrm{xc}}$, and $\Gamma_{\mathbf{k},n} = \Gamma_{\mathbf{k},n}^{\mathrm{qp}^{\gtrless}}$. The weight of (53) is reduced by the Debye-Waller-factor-like expression $\exp(-w_{\mathbf{k},n})$, whereas its nonvanishing imaginary part $\alpha_{\mathbf{k},n}$ gives rise to deviations of the spectral shape from a pure Lorentzian. The remaining spectral weight is shifted to the inelastic wings and satellite structure. Note also that, contrary to popular belief, owing to the short-time behavior (44) the wings of the spectrum far from the quasiparticle energy $E_{\mathbf{k},n}$ do not acquire a Lorentzian line shape. Moreover, in the case of electron promotion into the lowest unoccupied (or of hole into the highest occupied) band state $|\mathbf{k},n\rangle$, the threshold peak of the quasiparticle spectrum reduces to a δ function followed by the one-sided inelastic wing [16,36].

Exponential decay of the quasiparticle amplitude (48) cannot continue indefinitely in bands of finite width. Once the electron (hole) reaches the lowest unoccupied (highest occupied) level, its evolution collapses from exponential to power-law asymptotic decay [71]. This is illustrated in Fig. 2 of Ref. [72] and Fig. 10 of Ref. [36].

C. Temporal evolution of recoilless quasiparticles

For the behavior of $\rho_{\mathbf{k}}(\nu)$ around $\nu = 0$ that is different from that outlined in Sec. V B 2, the long-time limit of $C_{\mathbf{k}}(t)$ may acquire a nonlinear time dependence (cf. Sec. 3 of Ref. [36]). This, in turn, produces a profound effect on the quasiparticle spectrum (11). The most familiar case is the forward-scattering limit of recoilless quasiparticles arising from their infinite effective mass in flat bands so that $\epsilon_{\mathbf{k}-\mathbf{q}}^{0} - \epsilon_{\mathbf{k}}^{0} \simeq 0$. A classical example of such a reduction of the Hamiltonian (1) is provided by a core hole coupled to the continuum of incoherent e-h excitations constituting the system heat bath [18,52]. In this case the low-energy or infrared (IR) limit of the joint density of states (38) takes the form [16]

$$\rho_{\mathrm{IR}}(\nu) = \nu\left.\frac{\partial\rho}{\partial\nu}\right|_{\nu=0} = \alpha\nu, \quad \nu \leqslant \Omega_{\mathrm{IR}}, \tag{54}$$

where, due to the infinite mass of the source, the subscript $\mathbf{k}$ is omitted and Ω_{IR} denotes the cutoff parameter for the linear dependence in (54). Taking for calculational convenience the exponential form of the cutoff, $\exp(-\nu/\Omega_{\mathrm{IR}})$, we obtain an exact result,

$$C_{\mathrm{IR}}(t) = -i(\mp\alpha\Omega_{\mathrm{IR}})t - \alpha\ln(1 \pm i\Omega_{\mathrm{IR}}t), \tag{55}$$

where again the upper and lower signs refer to electrons (positive t) and holes (negative t), respectively. Substitution of (55) into (24) leads to the quasiparticle propagator

$$G_{\mathrm{IR}}(t) = \mp i\theta(\pm t)e^{-i\epsilon^{0}t}\frac{e^{\pm i\alpha\Omega_{\mathrm{IR}}t}}{(1 \pm i\Omega_{\mathrm{IR}}t)^{\alpha}}. \tag{56}$$

This exhibits the correct short-time limit (44), which is directly succeeded by the long-time limit of asymptotic power-law decay $\propto 1/t^{\alpha}$, i.e., without the passage through the stage of exponential decay $\propto \exp(-\Gamma t)$ characteristic of the recoiling quasiparticle regime described by Eq. (48). This is due to the absence of pole(s) from the FT of (56), whereby its (non)analytical properties arise exclusively from the cut along the positive (negative) real axis in the ω plane. This renders the spectrum exhibiting the IR power-law divergence at the excitation threshold

$$\mathcal{N}_{\mathrm{IR}}^{\gtrless}(\omega) = \frac{e^{-(\omega-\epsilon^{0}\pm\alpha\Omega_{\mathrm{IR}})/\Omega_{\mathrm{IR}}}\theta(\omega - \epsilon^{0} \pm \alpha\Omega_{\mathrm{IR}})}{\Omega_{\mathrm{IR}}^{\alpha}\Gamma(\alpha)(\omega - \epsilon^{0} \pm \alpha\Omega_{\mathrm{IR}})^{1-\alpha}}, \tag{57}$$

where $\Gamma(\alpha)$ is the Γ function, and α plays the role of critical exponent of the IR power-law divergence. A peculiar property of the spectrum (57) in comparison with (53) is the complete suppression of the elastic component at the quasiparticle threshold excitation energy (since the corresponding Debye-Waller exponent (DWE) is divergent, i.e., $\mathrm{Re}w_{\mathrm{IR}} \to \infty$ for $t \to \infty$) and the removal of the entire spectral weight to the IR divergent inelastic side wing.

D. Satellite structure in the quasiparticle spectrum

The joint density of excitations $\rho_{\mathbf{k}}(\nu)$ may embody, besides the quasiparticle component $\rho_{\mathbf{k}}^{\mathrm{qp}}(\nu)$ that is continuous around $\nu = 0$ and leads to (48), also the components that exhibit sharp peaks located at ω^{sat} away from $\nu = 0$ (cf. Fig. 3 in Ref. [76]), viz., that we have

$$\rho_{\mathbf{k}}(\nu) = \rho_{\mathbf{k}}^{\mathrm{qp}}(\nu) + \sum_{\mathrm{sat}}\rho_{\mathbf{k}}^{\mathrm{sat}}(\nu). \tag{58}$$

In electron gas such components $\rho_{\mathbf{k}}^{\mathrm{sat}}(\nu)$ may originate from plasmon modes of frequency $\omega_{\mathbf{q}}^{\mathrm{pl}}$. A prerequisite for the occurrence of a prominent peak in $\rho_{\mathbf{k}}^{\mathrm{sat}}(\nu)$ around $\nu = \omega^{\mathrm{sat}}$ is the small quasiparticle recoil energy $\epsilon_{\mathbf{k}}^{0} - \epsilon_{\mathbf{k}-\mathbf{q}}^{0} \ll \omega_{\mathbf{q}}^{\mathrm{pl}} \simeq \omega^{\mathrm{sat}}$. This gives rise to strong contributions from the oscillating term in the integrand on the RHS of (36), the so-called satellite generator, and produces contributions to $C_{\mathbf{k}}(t)$ oscillating with ω^{sat}.

1. Satellites in the plasmonic polaron model

To demonstrate the occurrence of satellite structures, we first introduce the simple plasmonic polaron model based on the ansatz for plasmon-pole(s)-dominated $\mathcal{D}^{\rm pl}_{\mathbf{q}}(\omega') = \frac{1}{\pi}|{\rm Im}\chi^{\rm pl}_{\mathbf{q}}(\omega')| = \mathcal{S}^{\rm pl}_{\mathbf{q}}\delta(\omega'-\omega^{\rm pl}_{\mathbf{q}})$. Here $\mathcal{S}^{\rm pl}_{\mathbf{q}}$ and $\omega^{\rm pl}_{\mathbf{q}}$ are the weight (residue) of a particular plasmon pole. In the limit of small recoil this leads to

$$\rho^{\rm sat\gtrless}_{\mathbf{k}}(\nu) = \sum_{\mathbf{q}} v^2_{\mathbf{k}-\mathbf{q},\mathbf{k}}\mathcal{S}^{\rm pl}_{\mathbf{q}}\delta\big[\nu-\big(\omega^{\rm pl}_{\mathbf{q}}\pm\epsilon^0_{\mathbf{k}-\mathbf{q}}\mp\epsilon^0_{\mathbf{k}}\big)\big]$$
$$\simeq w^{\rm sat}_{\mathbf{k}}\big(\omega^{\rm sat}_{\mathbf{k}}\big)^2\delta\big(\nu-\omega^{\rm sat}_{\mathbf{k}}\big), \tag{59}$$

in which the thus-defined $w^{\rm sat}_{\mathbf{k}}$ is generally strongly $\mathbf{k}$ dependent, whereas the $\mathbf{k}$ dependence of $\omega^{\rm sat}_{\mathbf{k}}$ is expected to be weak; i.e., $\omega^{\rm sat}_{\mathbf{k}}\simeq\omega^{\rm sat}$ as it originates from weakly dispersive $\omega^{\rm pl}_{\mathbf{q}}$. Substituting this into (37) we obtain

$$C^{\rm sat\gtrless}_{\mathbf{k}}(t) = -i\Delta^{\rm sat\gtrless}_{\mathbf{k}}t + w^{\rm sat\gtrless}_{\mathbf{k}}e^{\mp i\omega^{\rm sat}t} - w^{\rm sat\gtrless}_{\mathbf{k}}, \tag{60}$$

where

$$\Delta^{\rm sat\gtrless}_{\mathbf{k}} = \Delta^{\rm sat\gtrless}_{\mathbf{k}}(\epsilon^0_{\mathbf{k}}) \simeq \mp\sum_{\mathbf{q}}\mathcal{S}^{\rm pl}_{\mathbf{q}}v^2_{\mathbf{k}-\mathbf{q},\mathbf{k}}/\omega^{\rm sat}, \tag{61}$$

$$\Gamma^{\rm sat\gtrless}_{\mathbf{k}} = \Gamma^{\rm sat\gtrless}_{\mathbf{k}}(\epsilon^0_{\mathbf{k}}) = 0, \tag{62}$$

$$w^{\rm sat\gtrless}_{\mathbf{k}} \simeq \sum_{\mathbf{q}}\mathcal{S}^{\rm pl}_{\mathbf{q}}\left(\frac{v_{\mathbf{k}-\mathbf{q},\mathbf{k}}}{\omega^{\rm sat}}\right)^2 = \frac{|\Delta^{\rm sat\gtrless}_{\mathbf{k}}|}{\omega^{\rm sat}}. \tag{63}$$

Thereby each source peak in $\rho^{\rm sat}_{\mathbf{k}}(\nu)$ gives rise to the corresponding energy shift (61), the satellite generator $w^{\rm sat}_{\mathbf{k}}e^{\mp i\omega^{\rm sat}t}$, and the DWE (63), and they are all additive in $C_{\mathbf{k}}(t)$ and hence multiplicative in (24). Consequently, the spectrum (11) obtained from the FT of the product of $e^{-w^{\rm sat}_{\mathbf{k}}}$ and the expanded exponential $\exp(w^{\rm sat}_{\mathbf{k}}e^{\mp i\omega^{\rm sat}t})$ acquires the form of a series of discernible maxima or satellites located at integer multiples $\mp l\omega^{\rm sat}$ of the fundamental satellite frequency and weighted by $e^{-w^{\rm sat}_{\mathbf{k}}}(w^{\rm sat}_{\mathbf{k}})^l/l!$. Their shapes are given by the convolution of the narrow satellite-generating peak with the quasiparticle peak given by (53) or (57). In other words, each satellite peak in the spectrum (11) replicates the convolution with the structure of the quasielastic threshold peak [18,30]. Therefore, the quasiparticle spectrum in the plasmonic polaron model can be represented by a generic multiboson excitation expression frequently cited in the literature [17,18,23,35,52,77,78] (for generality we restore the band index n),

$$\mathcal{N}^{\gtrless}_{\mathbf{k}}(\omega) = \sum_{n,l=0}^{\infty} e^{-w^{\rm sat}_{\mathbf{k},n}}\frac{\big(w^{\rm sat}_{\mathbf{k},n}\big)^l}{l!}\mathcal{N}^{\rm qp\gtrless}_{\mathbf{k},n}\big(\omega-\epsilon^0_{\mathbf{k},n}-\Delta_{\mathbf{k},n}\mp l\omega^{\rm sat}\big), \tag{64}$$

where $\mathcal{N}^{\rm qp\gtrless}_{\mathbf{k},n}(\omega)$ is given by (53) and

$$\Delta_{\mathbf{k},n} = \Delta^{\rm qp}_{\mathbf{k},n} + \Delta^{\rm sat}_{\mathbf{k},n} \tag{65}$$

is determined from (51) and (61) or from a single calculation (45). The spectrum described by (64) follows the general pattern shown in Fig. 2. A completely analogous formula applies also in the limit of recoilless quasiparticles, in which case $\mathcal{N}^{\rm qp}(\omega)$ is replaced with $\mathcal{N}_{\rm IR}(\omega)$ [18,36,52]. Note that in the opposite limit, in which the quasiparticle recoil blurs the plasmon-induced satellite in $\rho^{\rm sat}_{\mathbf{k},n}(\nu)$ and gives rise

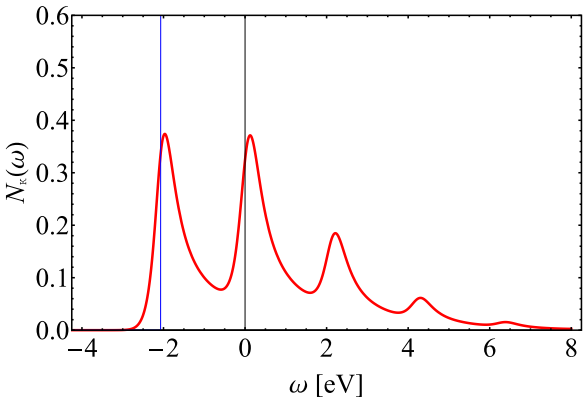

FIG. 2. Illustration of the quasiparticle spectrum $\mathcal{N}_{\mathbf{K}}(\omega)$ corresponding to propagation of a hot electron in an initially empty Q2D surface band completely above the Fermi level. The electron is coupled to the electronic charge density excitations in the underlying substrate whose spectrum consists of incoherent e-h pairs and surface plasmons of energy $\hbar\omega_s = 2$ eV. The calculation is performed for intermediate coupling strength and initial 2D electron momentum $K = 0.06$ a.u., which produces nearly equal strengths of the threshold and first satellite peak. The satellites appear approximately at multiples of the surface plasmon energy above the threshold energy $\epsilon_{\mathbf{K}} = \epsilon^0_{\mathbf{K}} + \Delta_{\mathbf{K}}$ of the leftmost peak (denoted by the vertical line at $\omega\simeq -2$ eV). Energy zero corresponds to the first moment of the spectrum which measures the energy shift $\Delta_{\mathbf{K}} < 0$ of the unperturbed level $\epsilon^0_{\mathbf{K}}$.

to $\Gamma^{\rm sat\gtrless}_{\mathbf{k}}(\epsilon^0_{\mathbf{k}}) > 0$, the regime described by Eq. (48) is also applicable to descriptions of excitation of real plasmons by the propagating quasiparticle (cf. Ref. [79] and Figs. 3 and 4 in Ref. [32]).

2. Satellites in ab initio GW + C approach

The situation becomes more complex when, instead of the plasmon-pole ansatz (59), the corresponding GW self-energy derived from first principles is used. In this case the satellite-generating component of $C^{(2)\gtrless}_{\mathbf{k},n}(t)$, which avoids overcounting of contributions leading to (48), reads

$$C^{\rm sat\gtrless}_{\mathbf{k},n}(t) = -\int d\nu\,\frac{\big[\rho^{(2)\gtrless}_{\mathbf{k},n}(\nu)-\rho^{(2)\rm qp\gtrless}_{\mathbf{k},n}(\nu)\big]}{\nu^2}(1-e^{\mp i\nu t})$$
$$= -w^{\rm sat\gtrless}_{\mathbf{k},n} + \mathcal{S}^{\rm sat\gtrless}_{\mathbf{k},n}(t), \tag{66}$$

where $\rho^{(2)\rm qp\gtrless}_{\mathbf{k},n}(\nu)$ is approximated with (47). Here the lth satellite in the quasiparticle spectrum is generated by the lth term in the expansion of $\exp[\mathcal{S}^{\rm sat\gtrless}_{\mathbf{k},n}(t)]$ in a power series. This requires calculations of the l-fold convolutions of the FT of $\mathcal{S}^{\rm sat\gtrless}_{\mathbf{k},n}(t)$ with the quasiparticle peak (53), and this is practically intractable for higher l's. However, since in the majority of systems of interest the quasiparticle coupling to plasmons is relatively weak (as measured by the effective $w^{\rm sat}_{\mathbf{k},n} < 1$ in practical applications only the first satellite need be computed. This is rather advantageous because the FT of

$\mathcal{S}^{\mathrm{sat}\gtrless}_{\mathbf{k},n}(t)$ is obtained in a simple form [30],

$$\mathcal{N}^{\mathrm{sat}\gtrless}_{\mathbf{k},n}(\omega)=\frac{\beta^{\gtrless}_{\mathbf{k},n}(\omega)-\left[\beta^{\gtrless}_{\mathbf{k},n}\left(\epsilon^0_{\mathbf{k},n}\right)+\left(\omega-\epsilon^0_{\mathbf{k},n}\right)\frac{\partial}{\partial\omega}\beta^{\gtrless}_{\mathbf{k},n}\left(\epsilon^0_{\mathbf{k},n}\right)\right]}{\left(\omega-\epsilon^0_{\mathbf{k},n}\right)^2}, \tag{67}$$

where $\beta^{\gtrless}_{\mathbf{k},n}(\omega)=\mp\frac{1}{\pi}\mathrm{Im}\Sigma^{(2)\gtrless}_{\mathbf{k},n}(\omega)$. Hence, the quasiparticle spectrum obtained by combining the *ab initio* G_0W_0 self-energy and cumulant approach takes the form

$$\mathcal{N}^{\gtrless}_{\mathbf{k}}(\omega)=\sum_n e^{-w^{\mathrm{sat}\gtrless}_{\mathbf{k},n}}\left\{\mathcal{N}^{\mathrm{qp}\gtrless}_{\mathbf{k},n}(\omega)+\mathcal{N}^{\mathrm{qp}\gtrless}_{\mathbf{k},n}(\omega)*\mathcal{N}^{\mathrm{sat}\gtrless}_{\mathbf{k},n}(\omega)+\mathcal{O}\left[\left(w^{\mathrm{sat}\gtrless}_{\mathbf{k},n}\right)^2\right]\right\}, \tag{68}$$

where $*$ denotes convolution. The quantitative difference between the spectra (64) and (68) computed for a concrete system is illustrated in Sec. VIII.

VI. CONNECTION OF CUMULANT EXPANSION WITH *GW* APPROXIMATIONS

Using expressions derived in Secs. IV and V, we are now in a position to assess the desired connection between the standard self-energy and cumulant expansion of the single-particle propagator (5) whose time evolution is governed by the dynamic interaction W (14). To this end we consider the regime of small but finite particle recoil in which the analytic properties of the renormalized propagator (12) are dominated by isolated simple poles, with only small contribution(s) from the cut(s). Thereby we avoid the limit (55) and allow for the appearance of distinct plasmon-generated peaks in the quasiparticle spectra. In this case we find that the long-time behavior of the second-order cumulant, which dominantly determines the quasiparticle spectral properties, is given by expressions (48) and (66). Their gross features should, according to (37), persist also in higher-order cumulants. This means that the temporal properties of the cumulant series, and thereby of ensuing $G_{\mathbf{k}}(t)$, are already determined by the G_0W_0-generated second-order cumulant (36). As pointed out in Ref. [17], this usually yields the best results for the physics of the unbound polaron problem described by (1).

Now, in view of the same form of integral representation of the general cumulant expression (37) and of the second-order term (36), it would be tempting to extrapolate the second-order result to the whole cumulant series (25) and replace it with expressions calculated from some higher-order terms of the GW self-energy $\Sigma^{\mathrm{GW}}_{\mathbf{k},n}(\omega)$. However, for the present problem defined by (1), this procedure is not justified and should be avoided. This is easily verified by examining the explicit forms of the next-higher, fourth-order cumulants $C^{(4)}_{\mathbf{k},n}(t)\propto\lambda^4$ that have been calculated for the present model [23,32]. The corresponding diagrams encompass the contributions with two noncrossing boson lines (GWA generic), two crossing boson lines (vertex corrections), and a product of two uncorrelated second-order corrections in the time domain (cf. Fig. 6.4 in Ref. [17]). All these terms are needed to construct the correct $C^{(4)}_{\mathbf{k},n}(t)$, whose long-time limit encompasses the on-the-energy-shell fourth-order Rayleigh-Schrödinger self-energy terms rather than solely the GWA-generated self-energy terms [17]. The same conclusion regarding the noncrossing and crossing boson line diagrams applies to higher-order cumulants [13] and thereby also to the whole cumulant series (25). This means that the replacement of the long-time limit of $C_{\mathbf{k},n}(t)$ in (25) by expressions deriving from self-consistent or higher-order $\Sigma^{\mathrm{GW}}_{\mathbf{k},n}(\omega)$ and its derivatives would first lead to erroneous terms that are nonlinear in t [17] and, second, to miscounting of the correlated self-energy corrections. This introduces spurious features in the quasiparticle propagator (24) and its spectrum (11).

The only exception to the above counterexample is the contribution represented by the generic G_0W_0 diagram of Fig. 1, which is common to both the second-order self-energy and cumulant series. Its two vertices are fully correlated through momentum conservation and in the long-time limit also through the energy conservation. For the present interaction W there is no subtraction of uncorrelated processes from the second-order cumulant and this leads to expressions (48) and (66). Therefore, if the second-order cumulant gives the dominant contribution to the series (25), as is the case in weakly correlated multiexcitation processes, then the results of G_0W_0 calculations can be efficiently exploited in the calculations of threshold and satellite properties of the spectra (11). In contrast, the use of GW approximation with G renormalized through some approximate or self-consistent form of self-energy $\Sigma^{\mathrm{GW}}_{\mathbf{k},n}$ going beyond the G_0W_0 level would give rise to unreliable results for G obtained from the cumulant representation (24).

Last, we note that in the calculations of optical response functions, i.e., the e-h pair propagators, the situation regarding the consistency of employing higher-order GW corrections for the one-particle propagators is different. Namely, here the inclusion of e-h vertex corrections calculated in the ladder approximation is consistent with the use of higher-order GW self-energies for the propagators [5], and this route has been followed in the calculations of optical properties of solids [80–84].

VII. PROTOCOL FOR IMPLEMENTATION OF THE *GW* + *C* APPROACH

In this section we summarize the results of this work in the form of a protocol for consistent implementation of *ab initio* GW and cumulant (GW + C) approach to the calculations of quasiparticle propagators and spectra. It encompasses several steps.

(i) The one-particle eigenstates $|\mathbf{k},n\rangle$ and eigenenergies $\epsilon^0_{\mathbf{k},n}$ that diagonalize the effective one-particle Hamiltonian (2) and define the band structure of the solid in the absence of screened interaction W are obtained using some well-established scheme. In practice, these are most often the Kohn-Sham (KS) one-particle states and energies calculated within the density-functional theory (DFT) employing a static (either local, semilocal or nonlocal) exchange and correlation potential $v_{\mathrm{xc}}(\mathbf{r})$.

(ii) Using the one-particle states and energies obtained in (i), the dynamic electronic response function $\chi_{\mathbf{q}}(\omega')$ of the system is calculated within the RPA or one of its improvements. From this one determines the excitation spectrum $\mathcal{D}_{\mathbf{q}}(\omega')$ needed in the calculation of the G_0W_0 quasiparticle self-energy defined in (16)–(18).

(iii) Following the arguments presented in Secs. IV and V and summarized in Sec. VI, the only justifiable consistent connection of the *ab initio* GW input and cumulant expansion can be established on the level of the G_0W_0 self-energy combined with the second-order cumulant. Otherwise, uncontrollable overcounting effects may be encountered. This GW + C procedure yields for quasiparticles in the Bloch states in the nth band

$$C^{\gtrless}_{\mathbf{k},n}(t) = -\int_{-\infty}^{\mu}{}^{\infty}_{\mu} d\omega' \frac{\mp\frac{1}{\pi}\mathrm{Im}\Sigma^{\gtrless}_{\mathbf{k},n}(\omega')}{\left(\omega' - \epsilon^0_{\mathbf{k},n}\right)^2}\left[1 - e^{-i(\omega'-\epsilon^0_{\mathbf{k},n})t}\right] - i\left[\mathrm{Re}\Sigma^{\gtrless}_{\mathbf{k},n}\left(\epsilon^0_{\mathbf{k},n}\right) - i v^{\mathrm{xc}}_{\mathbf{k},n}\right]t. \quad (69)$$

Here the upper and lower symbols refer to electron and hole, respectively, and $\Sigma^{\gtrless}_{\mathbf{k},n}(\omega')$ is the full G_0W_0 quasiparticle self-energy satisfying $\mp\mathrm{Im}\Sigma^{\gtrless}_{\mathbf{k},n}(\omega') \geqslant 0$. The second term on the RHS of (69) follows from Kramers-Kronig relations applied to the linear t term of $C^{\gtrless}_{\mathbf{k},n}(t)$ from which $v^{\mathrm{xc}}_{\mathbf{k},n}$ of Eq. (28) is subtracted if the unperturbed $|\mathbf{k},n\rangle$ and $\epsilon^0_{\mathbf{k},n}$ are the KS states and eigenenergies, respectively. Calculations of the ultrafast phenomena involving quasiparticle propagators should use this *nonasymptotic* form of the cumulants [33,34,44]. If the first term on the RHS of (69) is treated separately from the other terms, the factor $\pm i\eta$ may be added *ad hoc* into the denominator in order to remove spurious divergences from the expressions for satellite spectra.

(iv) Calculations of the quasiparticle spectra for comparison with the results of steady-state measurements (e.g., cw photoemission) may use the simpler long-time limit of (69) based on the ansatz used in (50). This enables carrying out the analytical treatment much farther and leads to the spectrum (68), whose practical implementation is demonstrated in Sec. VIII.

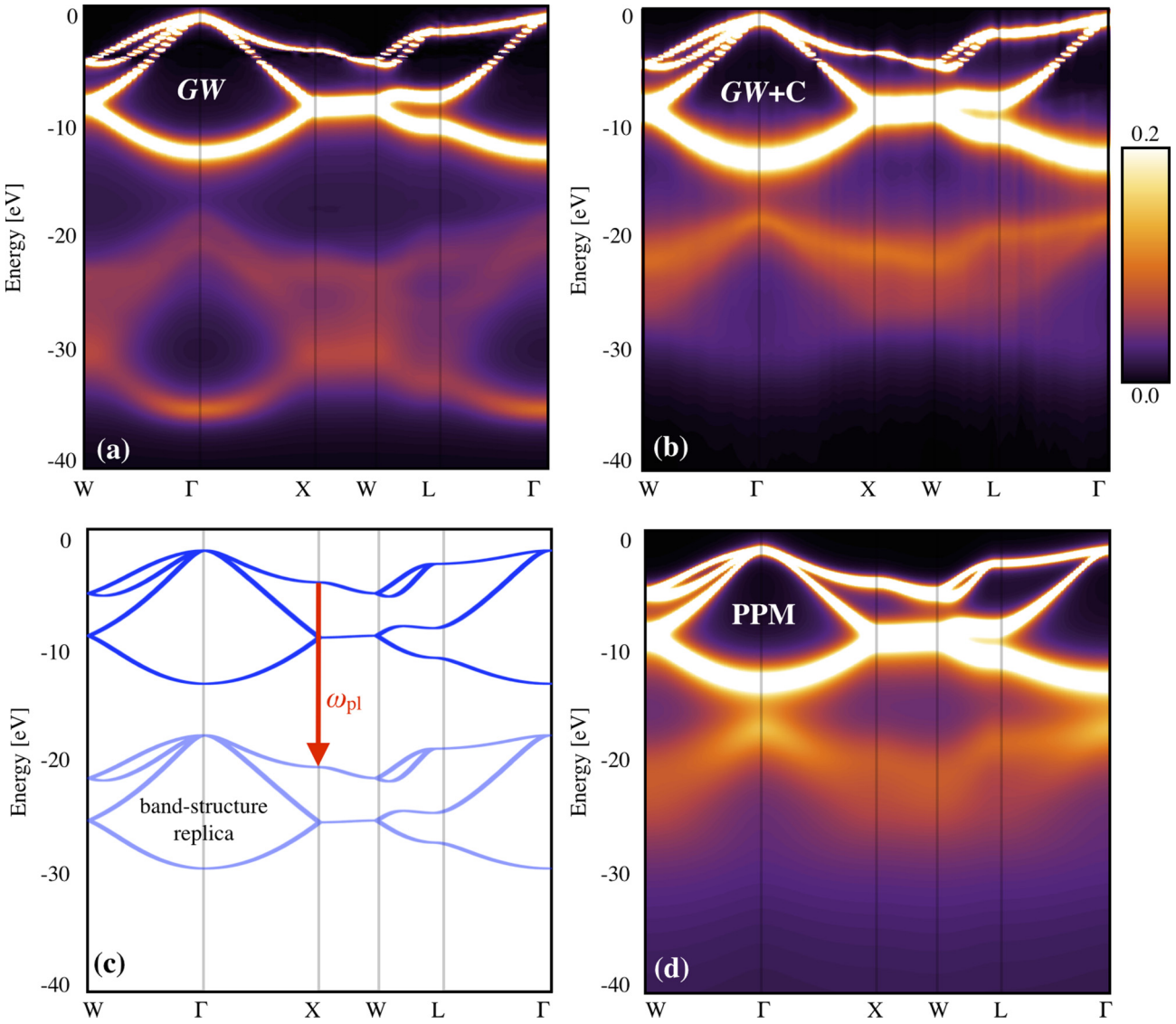

FIG. 3. Spectral function of silicon (in eV^{-1} units) evaluated using (a) the G_0W_0 approximation, (b) the G_0W_0 + cumulant (G_0W_0 + C) approach, (c) DFT-LDA, and (d) the plasmonic polaron model (PPM). For comparison, we report in panel (c) a replica of the DFT-LDA band structure redshifted by the plasmon energy ω_{pl} ($\omega_{pl} \simeq 16.6$ eV for silicon). All energies are relative to the Fermi level.

VIII. SPECTRAL FUNCTION OF SILICON VALENCE BANDS IN THE GW + C APPROACH

We now proceed to discuss the application of cumulant expansion in the context of *ab initio* calculations of spectral functions of solids. In particular, we study the spectral properties of silicon and the signatures of electron-plasmon interaction based on three different approaches: the G_0W_0 approximation, the $G_0W_0 + \mathrm{C}$ approach, and the plasmonic polaron model [43].

In the G_0W_0 approximation the spectral function is evaluated as

$$\mathcal{A}_{\mathbf{k}}(\omega) = \frac{1}{\pi}\sum_n \frac{\Sigma''_{\mathbf{k},n}(\omega)}{[\omega - \epsilon_{\mathbf{k},n} - \Delta\Sigma'_{\mathbf{k},n}(\omega)]^2 + [\Sigma''_{\mathbf{k},n}(\omega)]^2}, \tag{70}$$

where Σ' and Σ'' are the real and imaginary parts of the G_0W_0 self-energy, which we evaluate within the Sternheimer-GW approach [85,86]. $\epsilon^0_{\mathbf{k},n}$ denote Kohn-Sham DFT [87,88] eigenvalues in the nth band and $\Delta\Sigma'_{\mathbf{k},n}(\omega) \equiv \Sigma'_{\mathbf{k},n}(\omega) - v^{\mathrm{xc}}_{n\mathbf{k}}$, where $v^{\mathrm{xc}}_{\mathbf{k},n}$ is the exchange-correlation potential. The $G_0W_0 + \mathrm{C}$ spectral function has been obtained following the procedure leading to expression (68).

Finally, in the plasmonic polaron model the following approximations are introduced in order to circumvent the numerical cost of G_0W_0 calculations: (i) The quasiparticle linewidth is assumed to increase quadratically with the energy difference from the Fermi energy; (ii) the quasiparticle correction to the DFT eigenvalues are ignored; (iii) the imaginary part of the self-energy is approximated through a simple Lorentzian model. A detailed description of this procedure may be found elsewhere [43].

Density-functional theory calculations [87,88] in the Perdew-Zunger local density approximation (LDA) [89] are performed using the QUANTUM-ESPRESSO code [90]. We used a norm-conserving Troullier-Martins pseudopotential [91] and an 18-Ry kinetic energy cutoff to describe the wave functions. The Brillouin zone is discretized on a $6 \times 6 \times 6$ Monkhorst-Pack grid. The dielectric matrix of silicon has been evaluated using a 10-Ry kinetic energy cutoff, whereas we used an 18-Ry cutoff for the exchange part of the self-energy (see Eqs. (16)–(18) or Ref. [86] for the breakdown of the self-energy into its contributions from correlation and exchange). The frequency dependence of the screened Coulomb interaction was determined using a Padé approximant fit to 100 points along the imaginary frequency axis on a uniform grid from 0 to 25 eV. The Sternheimer-GW self-energy has been evaluated on a discrete frequency grid with a 25-meV spacing. The high-symmetry lines are computed with a momentum spacing of $0.025 \times 2\pi/a$, where $a = 10.26$ bohr is the lattice constant of silicon.

In Fig. 3(a), we show the G_0W_0 spectral function of silicon. At binding energies between 0 and 12 eV, the spectral function exhibits intense features which correspond to quasiparticle excitations in the absence of plasmons. These spectral features define the ordinary valence bands of silicon. At binding energies larger than 18 eV, the spectral function reveals additional spectral features with a well-defined dispersion that resembles that of the quasiparticle bands. These spectral features are

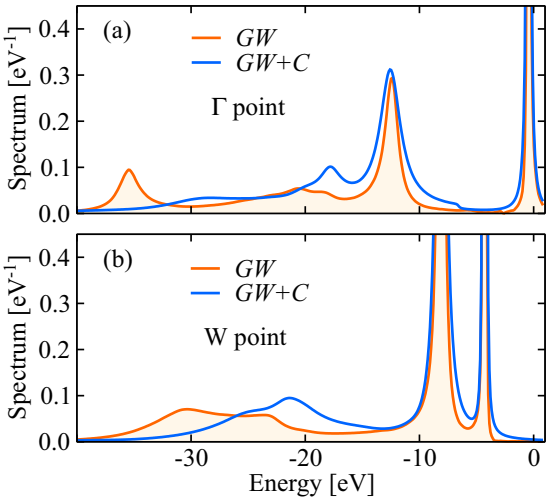

FIG. 4. Spectral function of silicon at the Γ (a) and W (b) high-symmetry points evaluated using the Sternheimer-GW method (G_0W_0 approximation) and the G_0W_0 + cumulant (GW + C) approach.

the band structures of plasmonic polarons [41,43] and stem from the simultaneous excitation of a hole and a plasmon. In the G_0W_0 approximation, plasmonic polaron bands are found at a binding energy of approximately 1.2–1.5ω_{pl} below the quasiparticle bands (in silicon $\omega_{\mathrm{pl}} \simeq 16.6$ eV). Overall, the G_0W_0 approximation overestimates the energy of these spectral features, which are typically found at $\sim\omega_{\mathrm{pl}}$ below the quasiparticle bands in photoemission experiment [42,46].

As compared to G_0W_0 calculations, the quasiparticle bands are left essentially unaffected by the $G_0W_0 + \mathrm{C}$ approach, as illustrated in Figs. 3(b) and 4. On the other hand, the plasmonic polaron bands are redshifted by $\sim\omega_{\mathrm{pl}}$ with respect to the quasiparticle bands, and are thus compatible with the energy range of plasmon satellite observed in X-ray photoemission spectroscopy (XPS) measurements [46]. To further emphasize the differences between the G_0W_0 and $G_0W_0 + \mathrm{C}$ spectral function, we compare in Fig. 4 the spectral function of silicon at the Γ and W high-symmetry points. Overall, the plasmonic polaron bands appear as a broadened low-intensity replica of the quasiparticle band structure, redshifted by the plasmon energy ω_{pl}. The prediction of plasmonic polaron band structures [41] was subsequently confirmed by angle-resolved photoemission spectroscopy experiments [42].

The spectral function obtained from the plasmonic polaron model [Fig. 3(d)] reproduces the main qualitative features of the $G_0W_0 + \mathrm{C}$ approach at a very small computational cost. As compared to $G_0W_0 + \mathrm{C}$ calculations, the plasmonic polaron bands appear slightly more smeared out as a consequence of quadratic dependence of the linewidth on the binding energy. For comparison, Fig. 3(c) reports the DFT-LDA band structure and a replica of the full valence band structure redshifted by the plasmon energy ω_{pl}.

IX. SUMMARY

It is argued that under the conditions of weakly correlated successive scattering events the propagator of a quantum particle (single electron or hole) in interaction with bosonized

excitations of the heat bath of a solid (single and collective electronic excitations, phonons, etc.) is obtained to a high level of accuracy from the second-order cumulant expansion. The second-order cumulant, which is proven to encompass the relevant dynamic features of the complete cumulant series (25), can be conveniently calculated from the corresponding G_0W_0-approximation expression for the quasiparticle self-energy [5,30,56]. The direct connection is established via Eqs. (34) and (35), which yield the G_0W_0-derived joint densities of excitations required to calculate the second-order cumulant (36). It is also emphasized that the use of higher-order forms of the GW approximation is not justified for the second- and higher-order cumulants. Thus, it is recommended that cumulant expansion be used in combination with the G_0W_0 approximation. Using silicon as a test case, we have illustrated the modifications of the quasiparticle spectral function which one obtains when moving from the standard G_0W_0 approximation to the more sophisticated cumulant expansion. We point out that the calculations are in good agreement with recent photoemission experiments [42].

The approach developed in the present work is rigorous in the limit of a quasiparticle propagating far above or below the Fermi level. However, the point at which it breaks down is system specific and could be estimated only by carrying out the standard Feynman-Dyson expansion of the same Green's function which enables the treatment of quasiparticle propagation in the vicinity of the Fermi level in both time directions (cf. discussion in Sec. III of Ref. [21] and in the last paragraph of Sec. IV D above). In this context, it appears that the formulation of Ref. [38] would interpolate smoothly between the G_0W_0 limits of our expressions for single electron and hole propagators (see also Sec. B of the Supplemental Material [68]); therefore, the present formulation and that of Ref. [38] should provide equivalent descriptions for quasiparticles far from the chemical potential. The equivalence of the two approaches close to the chemical potential is a more complex question because, as pointed out in Sec. IV D, in this case the second-order cumulant expansion breaks down, and the standard Feynman-Dyson perturbation expansion of the self-energy becomes more accurate [21]. We hope that this paper will stimulate further work on cumulant expansion and its applications to the studies of dynamical properties of quasiparticles in real materials and to the calculations of photoemission spectra.

ACKNOWLEDGMENTS

V.K. acknowledges partial support by the Croatian Science Foundation under Project No. 3526. F.C., H.L., and F.G. acknowledge support from the Leverhulme Trust (Grant No. RL-2012-001), the UK Engineering and Physical Sciences Research Council (Grant No. EP/J009857/1), the University of Oxford Advanced Research Computing (ARC) facility, and the ARCHER UK National Supercomputing Service.

[1] L. Hedin, Phys. Rev. **139**, A796 (1965).
[2] B. I. Lundqvist, Phys. Kondens. Mater. **6**, 193 (1967).
[3] M. S. Hybertsen and S. G. Louie, Comments Condens. Matter Phys. **13**, 223 (1987).
[4] A. G. Eguiluz, M. Heinrichsmeier, A. Fleszar, and W. Hanke, Phys. Rev. Lett. **68**, 1359 (1992).
[5] G. D. Mahan, Comments Solid State Phys. **16**, 333 (1994), and references therein.
[6] F. Aryasetiawan and O. Gunnarsson, Rep. Prog. Phys. **61**, 237 (1998), and references therein.
[7] W. G. Aulbur, L. Jönsson, and J. W. Wilkins, in *Solid State Physics*, edited by H. Ehrenreich and F. Spaepen (Academic Press, New York, 1999).
[8] L. Hedin, J. Phys.: Condens. Matter **11**, R489 (1999).
[9] B. Farid, in *Electron Correlation in the Solid State*, edited by N. H. March (World Scientific, Singapore, 1999), Chap. 3.
[10] G. Onida, L. Reining, and A. Rubio, Rev. Mod. Phys. **74**, 601 (2002), Sec. III and references therein.
[11] A. Marini, R. Del Sole, and A. Rubio, in *Time-Dependent Density Functional Theory*, edited by M. A. L. Marques, C. Ulrich, F. Nogueira, A. Rubio, K. Burke, and E. K. U. Gross, Lecture Notes in Physics Vol. 706 (Springer, Berlin, Heidelberg, 2006), Chap. 10.
[12] M. S. Hybertsen and S. G. Louie, Phys. Rev. B **34**, 5390 (1986).
[13] R. Kubo, J. Phys. Soc. Jpn. **17**, 1100 (1962).
[14] R. Brout and P. Carruthers, *Lectures on the Many-electron Problem* (Interscience, New York, 1963), Chap. 2.
[15] P. Nozières and C. T. De Dominicis, Phys. Rev. **178**, 1097 (1969).
[16] E. Müller-Hartmann, T. V. Ramakrishnan, and G. Toulouse, Phys. Rev. B **3**, 1102 (1971).
[17] G. D. Mahan, *Many Particle Physics* (Plenum, New York and London, 1981), Chap. 6.1.D.
[18] D. C. Langreth, Phys. Rev. B **1**, 471 (1970).
[19] D. C. Langreth, in *Collective Properties of Physical Systems* (Nobel Foundation, Stockholm, Sweden, 1973), Vol. 24, p. 210.
[20] G. D. Mahan, Phys. Rev. **145**, 602 (1966).
[21] S. Doniach, Phys. Rev. B **2**, 3898 (1970).
[22] J. J. Chang and D. C. Langreth, Phys. Rev. B **5**, 3512 (1972); **8**, 4638 (1973).
[23] D. Dunn, Can. J. Phys. **53**, 321 (1975).
[24] L. Hedin, Phys. Scr. **21**, 477 (1980).
[25] J. L. Skiner, J. Chem. Phys. **77**, 3398 (1982).
[26] D. Hsu and J. L. Skiner, J. Chem. Phys. **81**, 1604 (1984).
[27] C.-O. Almbladh and L. Hedin, in *Handbook on Synchrotron Radiation*, edited by E. E. Koch (North-Holland, Amsterdam, 1983), Vol. 1, Chap.8, Sec. 3.3.3.
[28] O. Gunnarsson, V. Meden, and K. Schönhammer, Phys. Rev. B **50**, 10462 (1994).
[29] F. Bechstedt, M. Fiedler, C. Kress, and R. Del Sole, Phys. Rev. B **49**, 7357 (1994).
[30] F. Aryasetiawan, L. Hedin, and K. Karlsson, Phys. Rev. Lett. **77**, 2268 (1996), and references therein.
[31] L. Hedin, J. Michiels, and J. Inglesfield, Phys. Rev. B **58**, 15565 (1998).
[32] B. Gumhalter, Phys. Rev. B **72**, 165406 (2005).

[33] P. Lazić, V. M. Silkin, E. V. Chulkov, P. M. Echenique, and B. Gumhalter, Phys. Rev. Lett. **97**, 086801 (2006).
[34] P. Lazić, V. M. Silkin, E. V. Chulkov, P. M. Echenique, and B. Gumhalter, Phys. Rev. B **76**, 045420 (2007).
[35] M. Guzzo, G. Lani, F. Sottile, P. Romaniello, M. Gatti, J. J. Kas, J. J. Rehr, M. G. Silly, F. Sirotti, and L. Reining, Phys. Rev. Lett. **107**, 166401 (2011).
[36] B. Gumhalter, Prog. Surf. Sci. **87**, 163 (2012).
[37] J. Lischner, D. Vigil-Fowler, and S. G. Louie, Phys. Rev. Lett. **110**, 146801 (2013).
[38] J. J. Kas, J. J. Rehr, and L. Reining, Phys. Rev. B **90**, 085112 (2014).
[39] J. Lischner, D. Vigil-Fowler, and S. G. Louie, Phys. Rev. B **89**, 125430 (2014).
[40] Y. Pavlyukh, A. Rubio, and J. Berakdar, Phys. Rev. B **87**, 205124 (2013).
[41] F. Caruso, H. Lambert, and F. Giustino, Phys. Rev. Lett. **114**, 146404 (2015).
[42] J. Lischner, G. K. Pálsson, D. Vigil-Fowler, S. Nemsak, J. Avila, M. C. Asensio, C. S. Fadley, and S. G. Louie, Phys. Rev. B **91**, 205113 (2015).
[43] F. Caruso and F. Giustino, Phys. Rev. B **92**, 045123 (2015).
[44] V. M. Silkin, P. Lazić, N. Došlić, H. Petek, and B. Gumhalter, Phys. Rev. B **92**, 155405 (2015).
[45] M. Guzzo, J. J. Kas, F. Sottile, M. G. Silly, F. Sirotti, J. J. Rehr, and L. Reining, Eur. Phys. J. B **85**, 324 (2012).
[46] M. Guzzo, J. J. Kas, L. Sponza, C. Giorgetti, F. Sottile, D. Pierucci, M. G. Silly, F. Sirotti, J. J. Rehr, and L. Reining, Phys. Rev. B **89**, 085425 (2014).
[47] J. S. Zhou, J. J. Kas, L. Sponza, I. Reshetnyak, M. Guzzo, C. Giorgetti, M. Gatti, F. Sottile, J. J. Rehr, and L. Reining, J. Chem. Phys. **143**, 184109 (2015).
[48] S. Engelsberg and J. R. Schrieffer, Phys. Rev. **131**, 993 (1963).
[49] A. A. Abrikosov, L. P. Gor'kov, and I. Ye. Dzyaloshinski, *Quantum Field Theoretical Methods in Statistical Physics* (Pergamon, Oxford, U.K., 1965), Chap. II.
[50] A. M. Zagoskin, *Quantum Theory of Many-Body Systems* (Springer-Verlag, New York, 1998).
[51] E. N. Economou, *Green's Functions in Quantum Physics* (Springer-Verlag, Berlin, Heidelberg, 2006).
[52] B. Gumhalter, Prog. Surf. Sci. **15**, 1 (1984).
[53] N. W. Ashcroft and W. L. Schaich, NBS Spec. Publ. (U. S.) **323**, 129 (1970); W. L. Schaich and N. W. Ashcroft, Phys. Rev. B **3**, 2452 (1971).
[54] C. Caroli D. Lederer-Rozenblatt, B. Roulet, and D. Saint-James, Phys. Rev. B **8**, 4552 (1973).
[55] Y. Takada and H. Yasuhara, Phys. Rev. Lett. **89**, 216402 (2002).
[56] J. J. Quinn and R. A. Ferrell, Phys. Rev. **112**, 812 (1958).
[57] B. Holm and U. von Barth, Phys. Rev. B **57**, 2108 (1998).
[58] A. Stan, N. E. Dahlen, and R. Van Leeuwen, Europhys. Lett. **76**, 298 (2006).
[59] C. Rostgaard, K. W. Jacobsen, and K. S. Thygesen, Phys. Rev. B **81**, 085103 (2010).
[60] F. Caruso, P. Rinke, X. Ren, M. Scheffler, and A. Rubio, Phys. Rev. B **86**, 081102 (2012).
[61] F. Caruso, P. Rinke, X. Ren, A. Rubio, and M. Scheffler, Phys. Rev. B **88**, 075105 (2013).
[62] E. P. Gross, in *Mathematical Methods in Solid State and Superfluid Theory*, edited by R. C. Clark and G. H. Derrick (Oliver and Boyd, Edinburgh, 1969), Chap. 2.3.
[63] S. Doniach and E. H. Sondheimer, *Green's Functions for Solid State Physicists* (W.A. Benjamin, New York, 1974).
[64] That such additional small expansion parameter may exist in the polaron problem was anticipated in Ref. [65].
[65] W. van Haeringen, Phys. Rev. **137**, A1902 (1965).
[66] X. Cui, C. Wang, A. Argondizzo, S. Garrett-Roe, B. Gumhalter, and H. Petek, Nat. Phys. **10**, 505 (2014).
[67] G. Giuliani and G. Vignale, *Quantum Theory of the Electron Liquid* (Cambridge University Press, Cambridge, U.K., 2005), p. 139.
[68] See Supplemental Material at http://link.aps.org/supplemental/10.1103/PhysRevB.94.035103 for a proof of the bijective integral representation and the ensuing drag-boson formulation of the cumulant series generated by the present particle-boson interaction..
[69] W. Brenig and B. Gumhalter, J. Phys. Chem. B **108**, 14549 (2004).
[70] D. K. Sunko and B. Gumhalter, Am. J. Phys. **72**, 231 (2004).
[71] L. A. Khalfin, Zh. Eksp. Teor. Fiz. **33**, 1371 (1958) [Sov. Phys. JETP **6**, 1053 (1958)].
[72] E. R. Fiori and H. M. Pastawski, Chem. Phys. Lett. **420**, 35 (2006).
[73] B. Gumhalter, A. Šiber, H. Buljan, and Th. Fauster, Phys. Rev. B **78**, 155410 (2008).
[74] S. Marion and B. Gumhalter, Phys. Stat. Solidi B **249**, 1218 (2012).
[75] P. Facchi and S. Pascazio, J. Phys. A: Math. Theor. **41**, 493001 (2008).
[76] T. McMullen and B. Bergersen, Can. J. Phys. **52**, 624 (1974).
[77] B. Gumhalter, A. Šiber, and J. P. Toennies, Phys. Rev. Lett. **83**, 1375 (1999).
[78] G. De Filippis, V. Cataudella, A. S. Mishchenko, C. A. Perroni, and J. T. Devreese, Phys. Rev. Lett. **96**, 136405 (2006).
[79] B. Gumhalter and D. M. Newns, Surf. Sci. **50**, 465 (1975).
[80] A. Marini and R. Del Sole, Phys. Rev. Lett. **91**, 176402 (2003).
[81] A. Marini, C. Hogan, M. Grüning, and D. Varsano, Comp. Phys. Commun. **180**, 1392 (2009).
[82] F. Bechstedt, K. Tenelsen, B. Adolph, and R. Del Sole, Phys. Rev. Lett. **78**, 1528 (1997).
[83] See Sec. IV B in Ref. [10].
[84] C. Attaccalite, M. Grüning, and A. Marini, Phys. Rev. B **84**, 245110 (2011).
[85] H. Lambert, F. Giustino Phys. Rev. B **88**, 075117 (2013).
[86] F. Giustino, M. L. Cohen, and S. G. Louie, Phys. Rev. B **81**, 115105 (2010).
[87] W. Kohn and L. J. Sham, Phys. Rev. **140**, A1133 (1965).
[88] P. Hohenberg and W. Kohn, Phys. Rev. **136**, B864 (1964).
[89] J. P. Perdew and A. Zunger, Phys. Rev. B **23**, 5048 (1981).
[90] P. Giannozzi *et al.*, J. Phys.: Condens. Matter **21**, 395502 (2009).
[91] N. Troullier and J. L. Martins, Phys. Rev. B **43**, 1993 (1991).